DOI: 10.1002/anie.201001451

Colloids

Colloidal Assembly: The Road from Particles to Colloidal Molecules and Crystals

*Fan Li, David P. Josephson, and Andreas Stein**

Keywords:
anisotropic particles · colloidal crystals · colloidal molecules · colloids · self-assembly

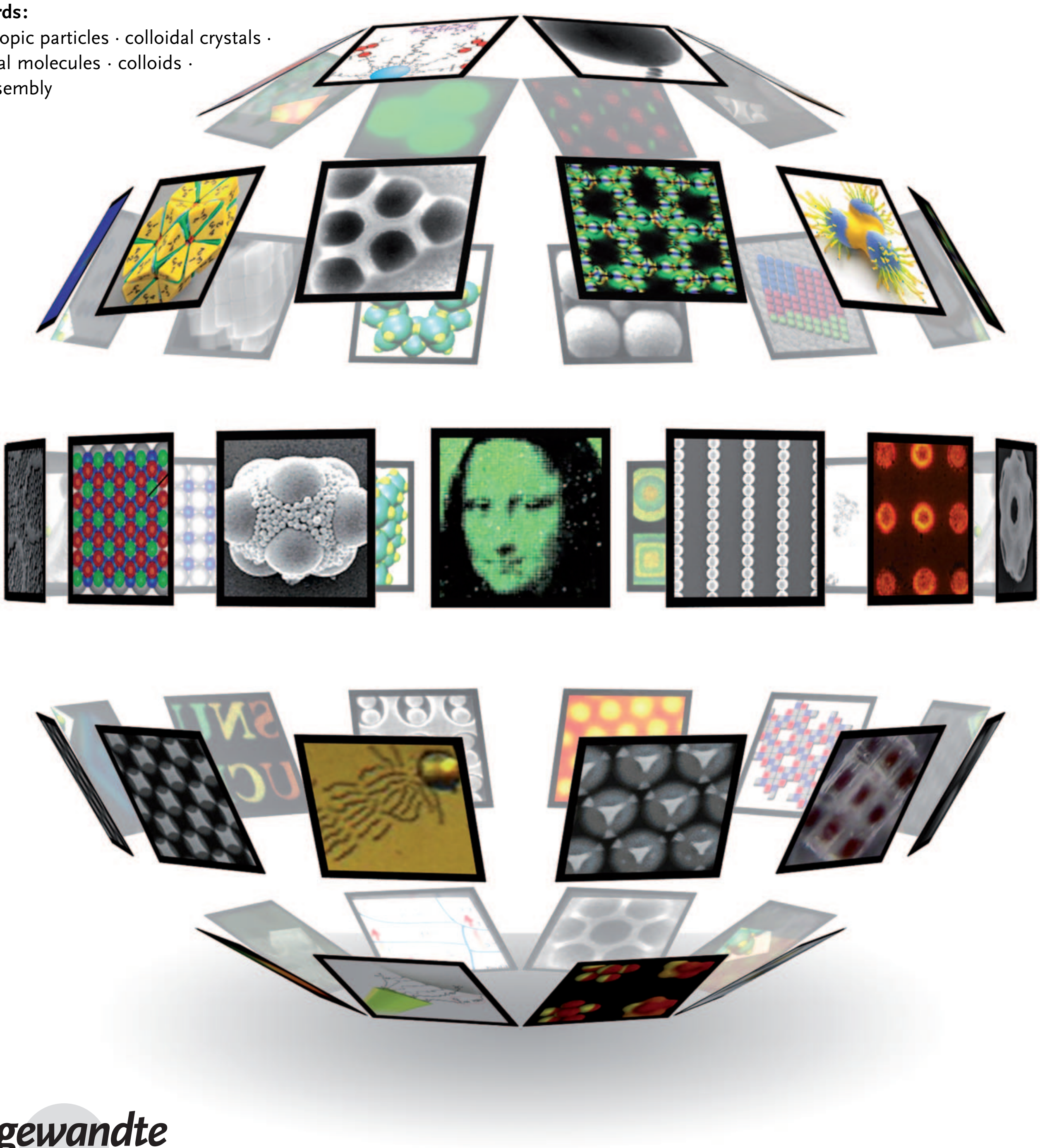

Colloidal particles may be considered as building blocks for materials, just like atoms are the bricks of molecules, macromolecules, and crystals. Periodic arrays of colloids (colloidal crystals) have attracted much interest over the last two decades, largely because of their unique photonic properties. The archetype opal structures are based on close-packed arrays of spheres of submicrometer diameter. Interest in structuring materials at this length scale, but with more complex features and ideally by self-assembly processes, has led to much progress in controlling features of both building blocks and assemblies. The necessary ingredients include colloids, colloidal clusters, and colloidal "molecules" which have special shapes and the ability to bind directionally, the control over short-range and long-range interactions, and the capability to place and orientate these bricks. This Review highlights recent experimental and theoretical progress in the assembly of colloids larger than 50 nm.

From the Contents

1. Introduction

> "*The principles of physics, as far as I can see, do not speak against the possibility of maneuvering things atom by atom. It is not an attempt to violate any laws; it is something, in principle, that can be done; but in practice, it has not been done because we are too big.*"
>
> Richard P. Feynman

While the scenario of manipulating chemical structures one atom at a time, as proposed by Prof. Feynman in 1959[**] still remains in its infancy 50 years later, the manipulation of colloidal spheres with shapes reminiscent of atoms, but a few orders of magnitude larger, has become an active territory for materials scientists. Owing to the structural similarities with atomic systems, colloidal assembly has served as an important model system to study the atomic world. For this purpose, intensive research has been conducted to tailor colloid sizes, shapes, surface properties, and interactions. This approach, inspired by the chemistry of atoms and molecules, has proven to be quite successful. Self-assembly of colloidal spheres in aqueous dispersion helped to clarify the early stage of crystallization in dilute solutions,[1] and self-assembly of binary nanoparticles into 3D ordered arrays also provided valuable insight for the construction of ionic crystals.[2]

The investigation of colloidal self-assembly as a means of nanostructure fabrication also holds technological implications. Colloidal structures prepared through self-assembly may find applications in, for example, photonic/plasmonic devices, nanoscale electronics, high efficiency energy-conversion/energy-storage, miniature diagnostic systems, drug/gene delivery, and hierarchically structured catalysts.[3] Compared to standard fabrication methods based on top-down approaches, such as optical lithography, colloidal self-assembly offers the potential for easier fabrication and manipulation of nano- and microstructures, especially in three dimensions. Currently this bottom-up approach is limited by the available building blocks, mostly isotropic, spherical particles. However, recent developments in syntheses of anisotropic colloids and "colloidal molecules", which offer the capability of bonding in specific directions, are starting to enhance the assortment of building blocks, and the construction of more intricate and perhaps more open structures assembled by colloidal units in the future can be foreseen.

Since the early work on monodisperse colloids with various shapes in the 1970s,[4] much progress has been made in both synthesis and self-assembly of colloidal particles of various sizes. In particular, the field of photonic crystals[5] boosted the interest in periodic arrays of colloidal particles, mainly spherical colloids with submicrometer to micrometer diameters.[6,7] Much progress has also been made in understanding the assembly of small nanoparticles (1–10 nm),[2,8] which may guide studies for larger colloids. However, interaction length scales differ for the two size regimes,

---

[*] Dr. F. Li,[+] D. P. Josephson, Prof. A. Stein
Department of Chemistry, University of Minnesota
207 Pleasant St. SE, Minneapolis, MN 55455 (USA)
Fax: (+1) 612-626-7541
E-mail: a-stein@umn.edu
Homepage: http://www.chem.umn.edu/groups/stein

[+] Current address: DuPont Central Research & Development
Rt 141 and Henry Clay, Wilmington, DE 19880 (USA)

[**] This statement is from Richard P. Feynman's classic talk "There's Plenty of Room at the Bottom" on December 29, 1959 at the annual meeting of the American Physical Society, California Institute of Technology. A transcript of the talk can be found under: http://www.zyvex.com/nanotech/feynman.html (accessed October 15, 2010).

nanoparticles being influenced by strong attractive van der Waals forces and by relatively long-range interactions compared to their sizes and larger colloids by short-range interactions relative to their dimensions.[9] Therefore the means to control assembly can be different for each regime. This Review will focus largely on the assembly of colloids with sizes over approximately 50 nm. After a brief synopsis of colloidal crystallization involving extended periodic structures, we will examine methods of guiding colloidal assembly in reduced dimensions or reduced symmetry to form colloidal analogues of molecules, clusters, and chains. We will highlight methods of creating and stabilizing particles that are anisotropic in shape or chemical functionality.[10] Concepts of directional assembly and cluster coupling will also be reviewed. The article concludes with considerations of theoretical studies and applications of colloidal assemblies.

2. Colloidal Crystallization

In cases where interparticle forces are sufficiently balanced in a colloidal system, self-assembly can occur. For example, monodisperse nanometer and micrometer sized spheres in a suspension can spontaneously form close-packed colloidal crystal arrays if their free volume is restricted below a certain level.[11] The surface charge of the particles must be sufficiently repulsive to discourage random aggregation but not large enough to prevent close packing.[12] The slight repulsive interactions between particles also allow them to rearrange into lower energy conformations as the free volume is decreased.[13] Spherical colloids typically pack into face-centered cubic (fcc), hexagonal close-packed (hcp), or random hexagonally close-packed (rhcp) arrays, fcc being entropically favored over hcp.[14]

Many different techniques including vertical deposition[15] and float packing[16] have been used to form colloidal crystals with fewer defects and larger crystalline domains. While these techniques have increased the quality and improved the fabrication time of the colloidal crystals, recent studies have made an effort to increase their mechanical stability and overall functionality.

A recently developed method to reduce crack formation during drying of a colloidal crystal film uses a photopolymer gel to immobilize the spheres in the loosely packed colloidal crystal film.[17] The free-standing film is then slowly shrunk using aqueous solutions containing increasing amounts of ethanol, which has a poor affinity for the gel polymer. This procedure avoids the inhomogeneous volume changes that are prevalent in air-drying methods and prevents cracking.

Colloidal crystal stability has also been improved by using a removable silica precursor in a suspension of silica spheres.[18] A tetraethyl orthosilicate (TEOS) precursor was added to the silica spheres and hydrolyzed. This procedure created a network of coarse silica in the interstitial spaces around the self-assembled silica spheres. The coarse silica was then etched out using hydrofluoric acid vapor. At certain TEOS concentrations, the interstitial course silica served to reduce the amount of shrinkage during drying and protected the colloidal crystal against cracking.

2.1. Influencing Self-Assembly by Modifying Particle Characteristics

While the fcc close-packed arrangement is thermodynamically favored for techniques using monodisperse, similarly charged spheres in suspension, other self-assembly methods can also be used to produce both close-packed and non-close-

Fan Li was born in Wuhan, China. He obtained a B.Sc. (2004) in Applied Chemistry and English from Tianjin University and his Ph.D. degree under the supervision of Prof. A. Stein (2010). He is currently a research investigator at DuPont Central Research and Development. His research interests include template-directed nanostructures and nanofabrication. He is the recipient of a Materials Research Society Graduate Student Silver Award (2007).

David Josephson obtained his B.S. degree in Chemistry at the University of North Dakota in 2007. He is currently pursuing his Ph.D. degree in Materials Chemistry under the supervision of Prof. A. Stein. His research interests include colloidal crystallization and photonic crystals.

Andreas Stein is a Distinguished McKnight University Professor at the University of Minnesota. He received his Ph.D. in Physical Chemistry from the University of Toronto in 1991 with G. A. Ozin and carried out postdoctoral research at Bayer A.G., Germany, the University of Texas and Penn State University (both with T. E. Mallouk). His research interests are in the field of solid-state chemistry, in particular porous materials, templating methods, and nanocomposites. He is the recipient of several awards, including a Merck Professorship, a DuPont Young Professor Grant, and an NSF CAREER Award.

packed arrays by altering particle characteristics, such as the size disparity, surface charge, geometry, or a combination of these factors.

2.1.1. *Adjusting Radius Ratios in Binary Systems*

Natural Brazilian opals contain a binary superlattice of two sizes of non-close packed silica spheres that are self-assembled into an ordered array.[19] Similar binary superlattices have also been synthetically fabricated using two sphere types with carefully controlled size ratios.[20] A relatively fast and simple method for preparing large-area, multilayered binary colloidal assemblies involves a horizontal deposition process.[21] By varying both number and size ratios between large and small polystyrene (PS) spheres, different packing configurations have been achieved. All configurations consisted of an fcc lattice of large spheres containing small spheres in the interstitial spaces. The small spheres were ordered into regular patterns on the surface of the colloidal crystal but exhibited reduced order further into the crystal.

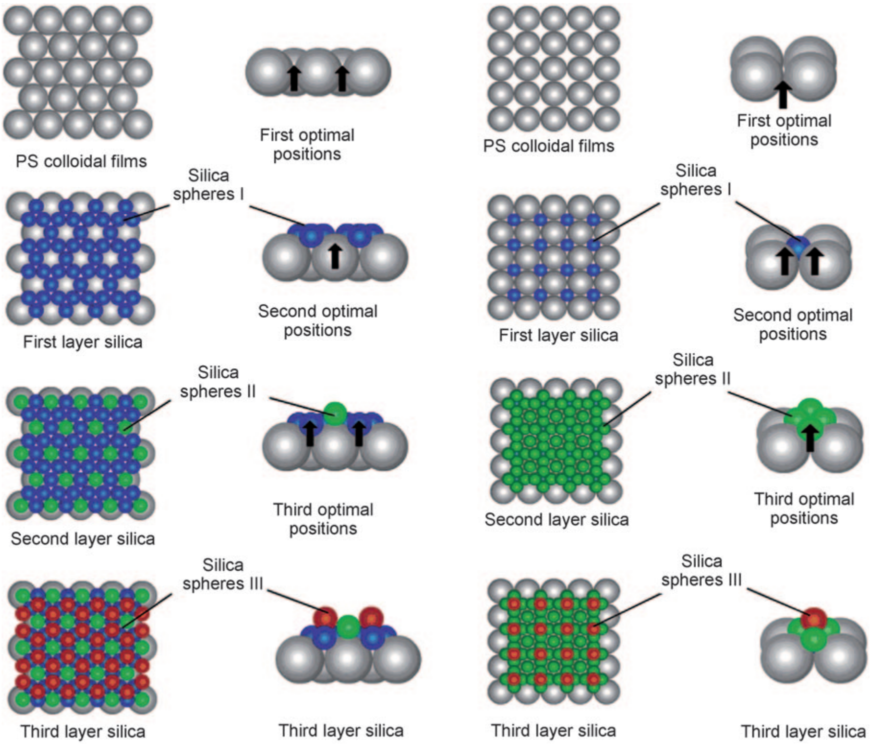

Figure 1. The packing mechanisms for small and large spheres into non-close-packed hexagonal (left) and rectangular structures (right). Reproduced with permission from Reference [22], copyright 2007, the American Chemical Society.

By using a sequential self-assembly method, non-close-packed silica arrays could be obtained.[22] Silica spheres having size ratios from 0.28–0.68:1 compared to PS spheres were deposited onto close-packed arrays of the PS spheres and became trapped in the void spaces between the larger PS spheres. Removal of the PS spheres by calcination exposed the silica packing structure at the PS sphere–silica sphere interface. The packing structure depended on the size ratio between the spheres, a ratio of 0.28:1 producing a disordered structure, 0.40:1 and 0.48:1 an LS_2 structure, and 0.68:1 an LS structure, where L represents large spheres and S small spheres (Figure 1). These structures were only observed at or near the interface with PS because, as multilayers of silica spheres were added, the spheres self-adjusted into close-packed arrays as if they had been grown on a flat substrate.

2.1.2. *Control through Electrostatic Interactions*

Electrostatic interactions play a large role in the self-assembly of particles into crystalline and non-crystalline arrays. Electrostatic interactions between particles may be altered to direct the formation of these arrays. For example, surface charges can be introduced on nanocrystals by the addition of a variety of capping groups, the charge on polymer spheres can be altered by the choice of polymerization initiators or added surface functionalization. Unique structures can also be prepared by invoking attractive interactions between spheres. However, these interactions must not be too strong or random aggregation may occur as a result of irreversible binding. If a crystalline, self-assembled structure of oppositely charged colloids is targeted, a delicate balance must be maintained between the entropically favored close-packed arrangements and the electrostatically driven non-close-packed structures.

While the ordering of close-packed spheres requires a sufficiently repulsive interaction between particles, the extent of that repulsion can be controlled through the use of amphoteric groups on the surface of the particles. Such groups introduce a pH-value-dependent surface charge, which allows both the sign and magnitude of the charge to be tuned. In the case of amphoteric PS spheres, colloidal crystals formed from a drop-cast suspension during solvent evaporation were more highly ordered when the surface charge on the particles was increased through adjustment of the pH value.[23] By adding an equal amount of oppositely charged silica spheres, it was possible to force weakly charged PS into a crystalline lattice.

Ionic colloidal crystals of oppositely charged particles have also been fabricated by taking advantage of the inherent surface charge of colloidal spheres.[24] Colloidal particles were dispersed in a density- and refractive-index-matched organic solvent to eliminate the influence of van der Waals forces. By varying the salt concentration of the colloidal suspension, it was possible to reverse the small charges on the particles. Utilizing the fact that different batches of synthesized poly(methyl methacrylate) (PMMA) and silica spheres had different charge reversal points, suspensions could be created that contained oppositely charged particles at a specific salt concentration. These particles spontaneously assembled into

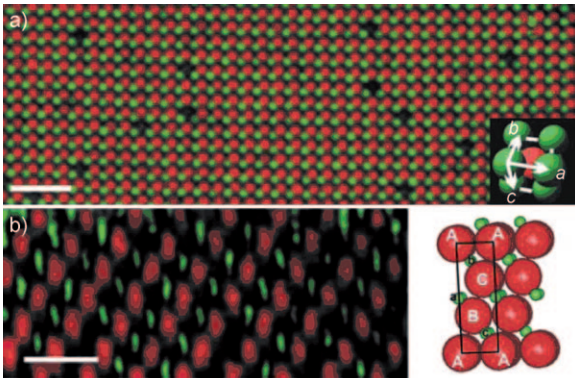

Figure 2. Confocal micrographs and models of a) a CsCl-type unit cell (scale bar = 10 μm) and b) an NaCl-type unit cell (scale bar = 8 μm). Reproduced with permission from Reference [24], copyright 2005, Nature Publishing Group.

a CsCl-type lattice (Figure 2a). At higher volume fractions, a randomly packed array was obtained. When particles of differing diameters were used, different structures were assembled based on the size ratios. Arrays with LS_6 and LS_8 stoichiometry, as well as NaCl (Figure 2b) and NiAs structures were obtained under separate conditions. The assembly of high-quality ionic colloidal crystals with long-range order, could be further facilitated by using a dielectrophoretic field to avoid gravitational separation of the binary colloids.[25]

The charge on colloidal particles can be further controlled by taking advantage of the polarity of added fluorescent dyes.[26] A binary mixture of nearly identical polymethylmethacrylate (PMMA) spheres was prepared with a nonpolar solvent that was both density and refractive-index matched. The two types of spheres were distinguished from one another by the presence of one of two types of cationic fluorescent dyes. The sphere charges were tuned by the addition of free bromide generated through the catalytic decomposition of cycloheptyl bromide by a length of ferromagnetic wire. Because the point of zero charge for each type of particle was different, given the separate polarities of the two dyes, the particle charge could be tuned near the zero charge point, where one type of particle underwent a charge inversion. The now attractive particles then self-assembled into ordered arrays. Using particles of similar size but opposite charge, rhcp, CsCl, and NaCl structures were obtained with successively increasing differences in particle charge.

Although the emphasis of this Review is on controlled assembly of larger colloids, important lessons may be learned from small-nanoparticle assembly. For self-assembled arrays of larger colloidal particles of differing charges, interparticle interactions tend to be short range with respect to the dimensions of the particle. This feature allows them to self-assemble more easily without aggregation. However, when very small nanoparticles are considered, the overall interaction forces are much more long range with respect to the particle sizes. This property leads to aggregation in systems with oppositely charged particles. Greater control over the extent of these forces is required to stabilize these smaller nanoparticle arrays.

If ordered, self-assembled structures of small, less than 10 nm, oppositely charged nanoparticles are targeted, more attention must be given to the degree of electrostatic interactions in the suspension. Thus, a reduction of the screening layer is necessary to avoid aggregation of the particles. This decrease may be achieved by using smaller nanoparticles to stabilize the larger ones in a process similar to Debye screening. A diamond-like structure was created when gold and silver nanoparticles (4–6 nm) were coated with functionalized alkane thiols to endow them with opposite charges.[27] When these particles were mixed, they assembled into ordered sphalerite arrays in which each nanoparticle was surrounded by four nanoparticles of opposite charge. The arrays spanned distances of a few microns.

Multiple binary superlattices have been assembled from small nanoparticles using a combination of sterically stabilized semiconducting, metallic, and magnetic nanoparticles.[28] It was demonstrated that the stoichiometry of the resulting self-assembled structures was established by the electrical charges on the sterically stabilized particles and that entropic, van der Waals, steric, and dipolar forces served to stabilize the arrays. Crystals of types AB, AB_2, AB_3, AB_4, AB_5, AB_6, and AB_{13} resembling NaCl, CuAu, AlB_2, $MgZn_2$, $MgNi_2$, Cu_3Au, Fe_4C, $CaCu_5$, CaB_6, and $NaZn_{13}$ structures self-assembled upon evaporation of solvent in a vertical assembly method. These self-assembled arrays were formed by tuning crystallite sizes and compositions (using combinations of oxides or other chalcogenides with metals) and modifying the surface charges of the nanoparticles with capping ligands.

2.2. Long-Range Self-Assembly of Nonspherical Particles

The shapes of colloidal particles also influence the packing patterns obtained through self-assembly. Different geometries of gold nanoparticles were assembled by solvent drop evaporation using concentrated aqueous dispersions of particles (Figure 3).[29] The particles were stabilized by

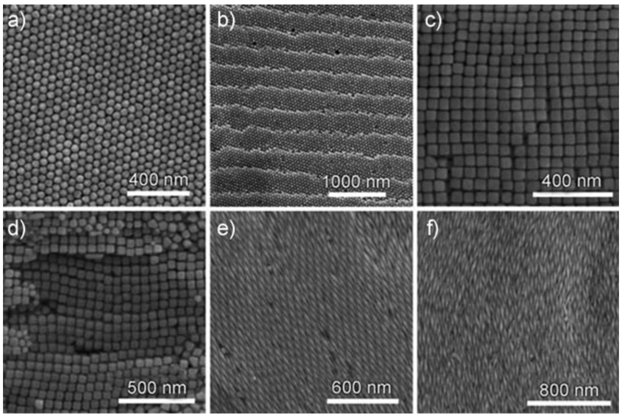

Figure 3. SEM images of ordered arrays of gold nanoparticles, including a) hexagonally packed Au polyhedra, b) hexagonally packed gold polyhedra with nearly periodic monosteps, c) tetragonally packed gold nanocubes, d) steps showing nanocubes in different layers, e) a superstructure formed from gold bipyramids and f) a nematic superstructure. Reproduced with permission from reference [29].

cetyltrimethylammonium bromide (CTAB) to balance the attractive depletion forces and the repulsive electrostatic forces and thus induce formation of ordered arrays during solvent evaporation without random aggregation. When gold nanorods were used, smectic and nematic liquid-crystal-like assemblies were obtained; gold polyhedra produced hexagonally packed structures; nanocubes produced tetragonal arrays; and bipyramidal shapes were found to form either nematic arrays or a 3D superlattice that had positional ordering in multiple directions (Figure 3). By combining nanorods with polyhedra in a binary mixture under precisely adjusted CTAB concentrations, the system organized into a non-close-packed rectangular lattice of polyhedra with nanorod arrays filling the interstitial spaces. Pentagonal silver nanoparticle rods have also been observed to self-assemble into densely packed arrays upon drying.[30] For rods with a length:diameter ratio of less than 4:1, the particles had a hexagonal packing structure over a long range despite their pentagonal geometry. The self-assembled layers of silver nanorods combined into a structure similar to a smectic mesophase.

Recently, a new approach to direct the assembly of oxide nanocubes to construct 3D simple cubic arrays was discovered. This unique route was based on using colloidal crystals as molds to control particle shapes and organization.[31] High quality colloidal crystals composed of PMMA spheres approximately 400 nm in diameter were infiltrated with a precursor solution for a mixed titania/phosphate glass phase. After removal of the polymer spheres, a three-dimensionally ordered macroporous (3DOM) structure formed initially, which, through controlled heating, spontaneously disassembled and evolved into individual particles with well-defined shapes.[32] Mediated by evaporation of the volatile phosphate phase, which possibly induced anisotropic capillary interactions,[33] the resulting nanocubes self-reassembled into simple cubic arrays (Figure 4). Such self-reassembly represents a simple and low-cost approach to realize long-range, non-fcc packing for large colloids, and has been successfully applied to several different metal oxide/phosphate systems.[34]

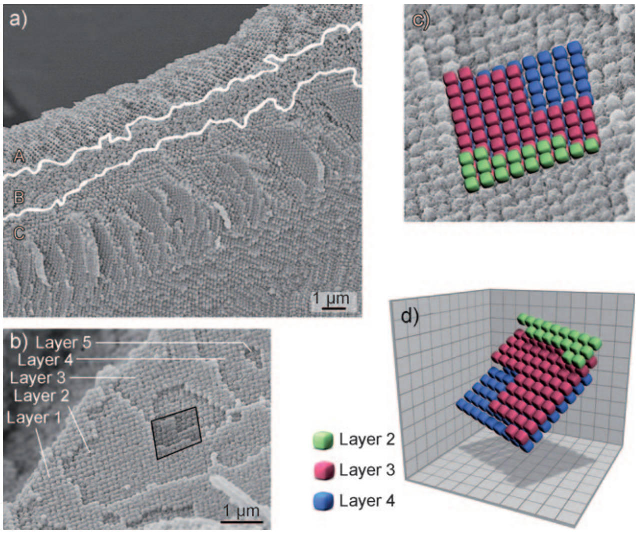

Figure 4. a) SEM image of a TiO_2/P_2O_5 sample (Ti:H_2O molar ratio = 1:1.8) prepared by self-reassembly. The image shows the transition from connected nanocubes (A), disconnected, randomly distributed nanocubes (B), to the largest region with simple cubic packing of nanocubes (C). b) SEM image of an ordered nanocube array with five discrete layers of square packing. c) An expanded view of the outlined region from (b) overlaid by colored cubes to illustrate the simple cubic packing. d) A three-dimensional plot of the three colored layers from (c). Reproduced with permission from Reference [32].

3. Guided Assembly

Just like cars in an assembly plant, colloidal particles can be assembled into specific arrangements one particle at a time by robotic manipulation. Robotic-like assembly of combined silica and PS spheres of equal diameter was demonstrated to construct a body-centered cubic photonic crystal with two interpenetrating diamond lattices on a patterned substrate.[35] In this case, PS spheres functioned as placeholders and were removed by oxygen plasma etching to leave a non-close-packed silica-sphere colloidal crystal with diamond symmetry. To assemble colloids in a more parallel fashion, self-assembly processes are desired. Specific patterns may be achieved by confinement and by guidance from internal and external forces.

Various interfacial phenomena have been exploited for the self-assembly of colloidal structures. Interfacial phenomena are particularly suitable for the synthesis of low-dimensional (0D–2D) structures, although on curved interfaces, they can be extended to three-dimensional structures. Herein we will discuss several representative methodologies that employ interfacial phenomena to assemble colloids. Colloidal assembly using external confinement will be discussed as well, because confinement also relies on interfaces to dictate the assembly.

3.1. Organization on a Patterned Substrate

The lattice structure and orientation of a colloidal crystal can be predefined by colloidal epitaxy, that is, sedimentation of microspheres on lithographic patterns that direct the growth of the first layer.[36] Structural order in this technique is limited to the first few layers adjacent to the substrate. In pre-patterned surfaces prepared, for example, by soft lithography, colloidal spheres assemble into arrays whose order depends closely on the relative dimensions of the spheres and the pattern as well as the pattern geometry.[37] Confinement effects offer a versatile approach to control colloidal particle assembly into low-dimensional structures. Spheres may be spin-coated over patterns, such as microwell arrays and V-shaped line patterns.[38,39] During this process, combined gravitational and capillary forces present during sedimentation and dewetting cause the colloidal particles to self-assemble into colloidal crystals within the etched patterns. In V-shaped line patterns, straight and helical arrangements of spheres are possible, depending on the sphere diameter relative to the line width and the V-angle.[38] The handedness of helical structures may be controlled by adjusting the orientation of capillary forces during dewetting of the aqueous suspension of PS spheres relative to the direction of the V-grooves. Free-standing, helical chains or self-supporting 2D arrays can be obtained after annealing the PS beads and releasing them from the grooves or microwells. By varying the ratios of the sphere diameter to the pattern dimensions, it is possible to form 2D superstructures, including those analogous to graphite, kagome, bcc, open hexagonal and tetragonal structures.[39]

Although surface assembly by confinement is typically performed in a liquid where particle organization is driven by capillary forces,[40] alternate approaches involving a dry state exist. In a recent study, a dry manual assembly process was developed in which colloids were placed into hole patterns by mechanical rubbing. As a result of the strong rubbing force, this manual assembly approach permits assembly of colloids guided by holes that are smaller than the colloid sizes (Figure 5).[41]

Non-close-packed 2D arrays of particles can be obtained by depositing hydrogel particles loaded with $CaCO_3$ on a surface and allowing these to shrink during drying.[42] Smaller particles may be packed around the non-close-packed particles in another dip-coating step, forming superhydrophobic surfaces of irregularly packed binary colloidal assemblies.

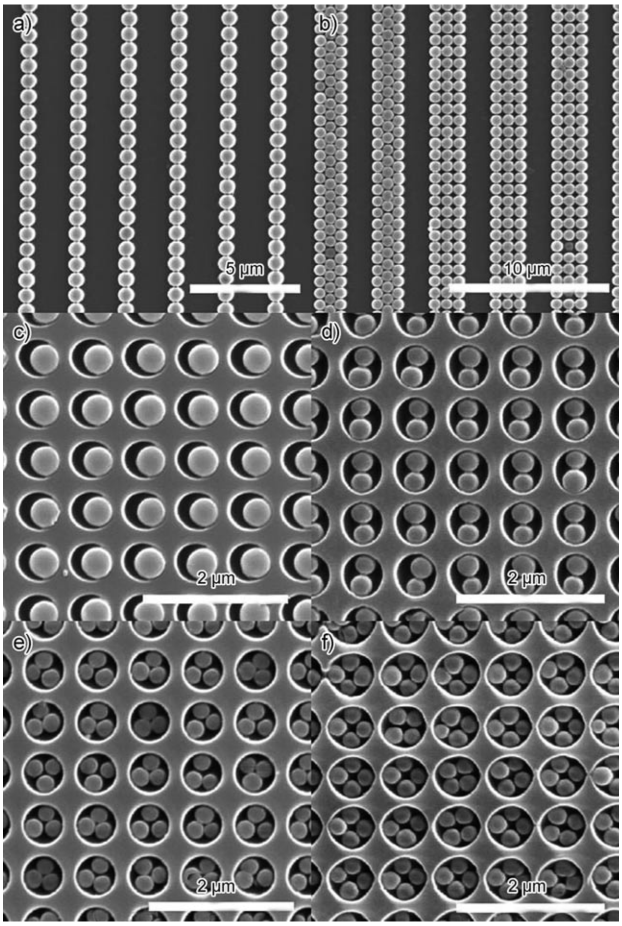

Figure 5. Colloidal chains and clusters prepared by dry manual assembly (rubbing). a), b) Single-particle or multiple-particle colloidal chains. c)–f) Colloids and clusters inside cylindrical holes. Reproduced with permission from Reference [41], copyright 2009, the American Chemical Society.

To assemble monolayers of colloidal particles in specific patterns, a substrate does not necessarily require a depth component arising from indentations, wells, or grooves. Instead, it is possible to use chemical patterns that guide the assembly based on electrostatic interactions or hydrophilic/hydrophic interactions. Complex patterns on the micrometer length scale can be generated by stamping polyelectrolyte layers onto a substrate and using these to guide the assembly of charged colloidal particles (Figure 6).[43,44]

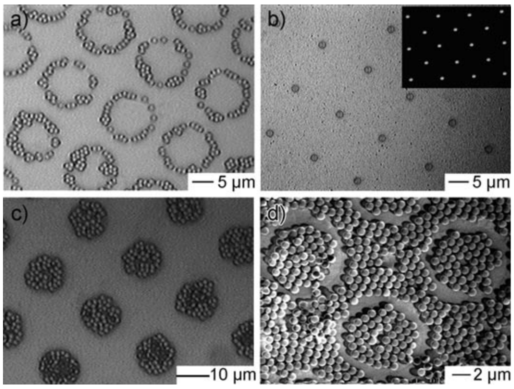

Figure 6. Optical microscope and SEM images of PS sulfate latex particles on substrates patterned with polyelectrolytes. a) Ring patterns, b) dot patterns (insert: dark-field image of single particle array), c) circular patch patterns, d) out-of-ring patterns. Reproduced with permission from Reference [43], copyright 2002, the American Chemical Society.

Surface patterns have also been generated by site-specific plasma oxidation of a polydimethylsiloxane (PDMS) substrate through screen masks.[45] This process converted regions of the hydrophobic $SiCH_3$ terminated surface to areas with more hydrophilic SiO_x surface groups and generated a pattern of hydrophobic/hydrophilic domains on the substrate. When the substrate was coated with a colloidal suspension, droplets of the suspension were drawn from hydrophobic to hydrophilic domains during drying, forming ordered colloidal assemblies. The most ordered assemblies were obtained if ethanol was added to the aqueous suspensions to reduce the surface tension and enhance the evaporation rate.

3.2. Langmuir–Blodgett Assembly

Amphiphilic molecules preferably reside at an oil-and-water interface, where they can form a molecular monolayer at appropriate concentrations. This characteristic is exploited in the Langmuir–Blodgett technique, in which a vertical lifting plate is used to retrieve the monolayer film from the interface. This technique was recently extended to manipulate colloids using a similar mechanism: an oil dispersion of nanocrystals or colloids was deposited onto a liquid surface, and manipulation of the particle monolayer by compression or expansion resulted in different assembly patterns at the interface (Figure 7a).[46] The colloidal pattern could then be

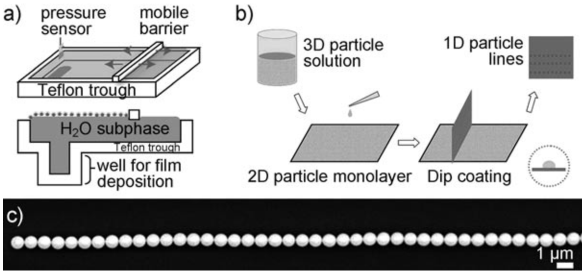

Figure 7. Langmuir–Blodgett technique for colloidal assembly. a) Illustration of a Langmuir–Blodgett trough. b) Process of assembling 1D colloidal arrays from a dilute monolayer. Particle strings are produced at the contact line formed by the intersection of the vertical substrate with the plane of a floating colloidal-particle monolayer. c) SEM image of a 1D colloidal array. Reproduced with permission from Reference [46], copyright 2008, the American Chemical Society.

transferred onto a substrate. However, depending on the affinity for the liquid phase, the substrate also influenced the resulting patterns. Governed by a series of factors (e.g., surface pressure, substrate hydrophobicity, and pulling speed), the colloids could be arranged into continuous or scattered colloidal strings, oriented either perpendicular[47] or parallel[48] to the liquid surface (Figure 7b,c). The interchain and interparticle spacing was tailored by the pulling speed and the nanoparticle density.[49]

3.3. Surfactant-Assisted Assembly

Colloids can self-assemble into strings or extended networks in an aqueous solution of a non-ionic surfactant, where the surfactant forms a *meso*-scale liquid crystal. A systematic study of the spatial localization of silica colloids in a hexagonal surfactant mesophase revealed that, while small colloids could be easily incorporated into the mesophase (as indicated by the expansion of the *d*-spacing), larger colloids were excluded.[50] In addition, it was found that the exclusion of large colloids prompted these to form assembled phases in the vicinity of the mesophase, and this phenomenon was applied to develop a colloidal-assembly strategy in a surfactant liquid crystal (Figure 8).[51] In certain cases, the presence of a liquid-crystal mesophase was not required, as 1D silica nanoparticle (NP) strings were also observed in a mixture of silica particles and the surfactant Pluronic F127 ($PEO_{100}PPO_{70}PEO_{100}$ PEO = polyethyleneoxide, PPO = polypropylene oxide), in which no columnar mesophase was detected. This result suggested that the assembly may also be engaged by a synergistic effect, perhaps by hydrogen bonding between colloids and surfactant molecules.[52] Similarly, CdSe/CdS core–shell colloids that bear a brush-like PEO layer self-assembled into chain-like structures or three-dimensional vesicular aggregates when the surface PEO density was varied. It was suggested that, while a complete PEO coating stabilized the colloids, insufficient amounts of PEO and moderate binding with the nanocrystal surface caused dynamic re-arrangement and introduced certain amphiphilic properties into the colloids, which led to their self-assembly.[53] In addition, it was suggested that the combination of macromolecules and colloids could not only facilitate colloidal assembly, but perhaps be utilized to create anisotropic functionalities,[54] setting the stage for exploration of reversible attachment of tailored surface moieties for controlled assembly and disassembly of nanoparticles.[55]

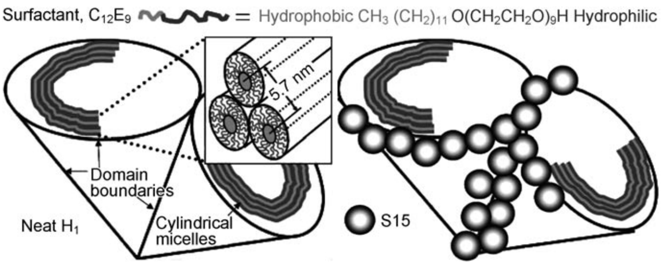

Figure 8. The spatial localization of colloidal particles by surfactant micelles (right). Features of the neat surfactant phase (H_1) are defined in the left panel. S15 refers to 15 nm sized silica nanoparticles. Reproduced with permission from Reference [51], copyright 2009, the American Chemical Society.

3.4. Assembly in Nematic Liquid Crystals

Colloidal assembly in nematic liquid crystals (NLC) is highly interesting because of the induced anisotropic interactions.[56] A NLC is an orientationally ordered, complex fluid formed by rod-shaped molecules that are aligned along a common direction. When colloids are immersed in a NLC, the uniform alignment of the surrounding nematic phase is disturbed. Depending on the colloid size, the type and strength of surface anchoring, and the size of the confinement, point or line defects may be induced through elastic distortion at the nematic–particle interface (Figure 9a).[57] For spherical colloids, this introduces two basic types of anisotropy in the colloid surface, either dipolar or quadrupolar symmetry. The

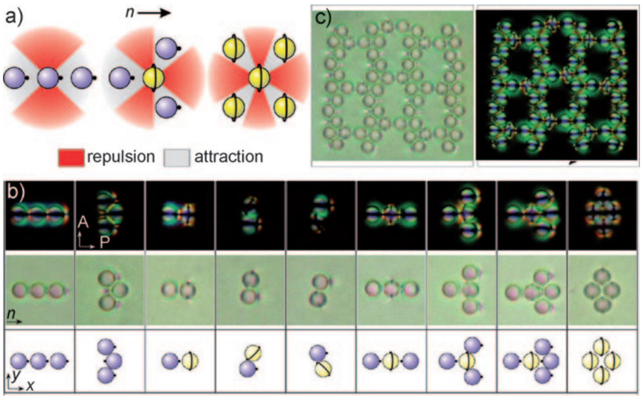

Figure 9. Colloidal spheres in nematic liquid crystals. a) Illustration of angle-dependent interactions between dipolar and quadrupolar colloidal particles. *n* = direction of alignment of NLC. b) Basic arrangement of dipolar and quadrupolar colloid clusters: polarized (top row) and unpolarized (middle row) images and corresponding illustrations (bottom row). A,P = directions of the analyzer and polarizer. c) Unpolarized (left) and polarized (right) images of complex pattern formed by binary colloids. Reproduced with permission from Reference [59], copyright 2009, the American Chemical Society.

total free energy of elastically distorted nematic liquid crystals can be minimized when approaching colloids are arranged in a defined orientation and separation, which makes them capable of directional assembly. Therefore, through carefully controlling these interactions, it is possible to envision chemistry on the colloidal level, that is, synthesis of colloidal molecules with specific geometries.[56] The possible assembly patterns of colloids within a nematic host have been studied. Two basic configurations are linear chains of dipolar colloidal particles and kinked chains developed by quadrupolar colloids.[57] In addition, when the two types of nematic colloids are combined, more complex assembly patterns can be achieved. The mixed interactions in this system greatly expand the range of attainable colloidal structures.[58] Colloidal clusters formed by combining a number of binary nematic colloids may be further employed as "building blocks" for the assembly of even more complex structures (Figure 9 b, c). Such complexity begins to resemble chemistry at a molecular level.[59]

More structural variety results from non-spherical colloids. When equilateral polygonal platelets were placed in a NLC, distinct field-directed configurations were obtained, which were visualized by the addition of an anisotropic fluorescent dye to the NLC (Figure 10). The polarity depended on whether the number of sides of the platelets was odd or even.[60] Although the final structures were indeed thermodynamically stable under the elastic colloidal forces in the NLC, the assembly was made possible by using optical tweezers to place the colloids. Pathways for self-assembly from complete randomness to highly ordered structures in NLC have not yet been discovered for complex mixed colloids.

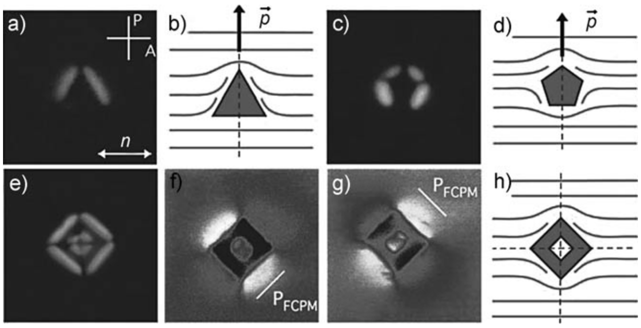

Figure 10. Shaped colloids in nematic liquid crystals.[60] A, P = directions of the analyzer and polarizer. n = direction of alignment of NLC, P_{FCPM} = direction of the linear polarizer in the fluorescence confocal polarizing microscope, vector $\vec{p}$ = dipole moment direction. a), c), e) Polarizing microscopy images of triangular, pentagonal and square colloids in NLC. b), d), h) Illustrations of director field configurations around triangular, pentagonal, and square colloids. f), g) Fluorescence confocal polarizing microscopy images of square colloids in two different configurations. Reproduced with permission from Reference [60], copyright 2009, the American Association for the Advancement of Science.

3.5. Assembly in Emulsions or Inverse Emulsions

Colloidal spheres can assemble themselves at the interface of emulsion droplets present in a blend of immiscible fluids to form spherical shells, so called colloidosomes.[61–63] The spheres tend to close-pack at the interface, but due to the curvature, the packing is not as homogeneous as in planar systems. Annealing of such colloidosomes slightly above their glass transition temperature produces selectively permeable capsules. One component in the emulsion may contain guest species, which can permeate through the interstitial space between spheres. Besides annealing, it is also possible to use electrostatic or van der Waals forces to lock colloidal particles together at the interfaces. As a result of the distribution of emulsion droplet sizes, the products contain multiple "cluster" sizes, which need to be separated to form sets of uniform clusters. Less polydisperse clusters may be obtained by assembly around emulsion droplets or gas bubbles in microfluidic devices.[64,65] An interesting approach used monodisperse CO_2 bubbles generated in an aqueous dispersion of anionic colloidal particles in a microfluidic T-junction device. As these bubbles dissolved, they shrunk and lowered the solution pH value. At the same time, carboxylate groups on the anionic particles were protonated and the particles adsorbed at the gas–liquid interface to form "armored bubbles", that is, hollow spheres with colloidal particle shells. The process relied on the pH-value-driven changes in surface energies and did not occur with nitrogen bubbles.[65]

When fewer colloidal spheres are confined within each emulsion droplet, densely packed colloidal clusters can be formed following the evaporation of the liquid. In this case the high packing density and symmetry of the polyhedral clusters is driven by capillary forces during the evaporation,[66] and the cluster configurations appear to be dictated by minimization of the second moment of the mass distribution in the cluster.[63] Typically, mixed clusters containing different numbers of colloidal spheres are generated during the emulsification process, therefore requiring further separation. However, several techniques have been developed to produce nearly monodisperse clusters.[64,67]

By combining colloidal microspheres (silica, PS) with smaller nanospheres (silica, titania) in oil-in-water emulsions, composite clusters are formed whose geometries depend on the larger colloids, whereas the small nanoparticles only fill the voids (Figure 11 a, b). After removal of PS spheres by calcination, hollow particles with interesting geometries are obtained (Figure 11 c).[68]

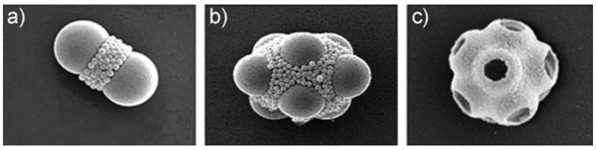

Figure 11. Composite colloidal clusters. a), b) Composite clusters formed by binary colloids in water droplets. c) Hollow silica cell after the PS was removed from a silica–PS composite cluster. Reproduced with permission from Reference [68], copyright 2005, the American Chemical Society.

Colloidosome assembly on the surface of temperature-sensitive microgel scaffolds in water-based emulsion systems produces shell structures whose permeability is controllable by temperature.[62] In one example, negatively charged PS spheres were adsorbed on much larger positively charged poly(*N*-isopropylacrylamide) microgel particles through Coulombic interactions. When the microgel particles shrank at higher temperature, they brought the PS spheres closer together and eventually caused buckling of the PS layer to produce irregularly shaped colloidosomes.

3.6. Assembly in Fibers and Cells

One dimensional confinement of colloidal particles is possible within groove and channel patterns of a substrate,[69] but can be extended to larger length scales by confining particles within polymer nanofibers. The extent of guiding by confinement depends on the particle–polymer interactions. In the case of silica spheres dispersed in polymer solutions that were electrospun into fibers, particles were confined in the polymer if the polymer wetted the particles well.[70] For large ratios of silica-sphere-diameter to polymer-nanofiber-diameter, single particle strings were formed; for smaller ratios, less-ordered, close-packed particle arrays formed. Extension of the fibers also induced the particles to assemble into pearl-necklace structures. Calcination eliminated the polymer matrix, leaving colloidal silica strands. For polymers that did not wet the spheres well, these spheres were found at the polymer/air interface after electrospinning.

To achieve higher dimensionality, micron-sized particles ingested by a fibroblast cell were crystallized into 2D and 3D close-packed arrays, guided by confinement in the cell membrane and by repulsive inter-particle interactions (Figure 12).[71] Random motions by the cytoskeleton produced forces stronger than thermal forces and helped to eliminate defects in the colloidal crystal. In mixtures of uniform large and small particles, the smaller particles were driven to the perimeter of the colloidal assembly. Particles with diameters of 500 nm or less did not form colloidal crystals, possibly a result of the diminished confinement effects of the curved cell membrane.

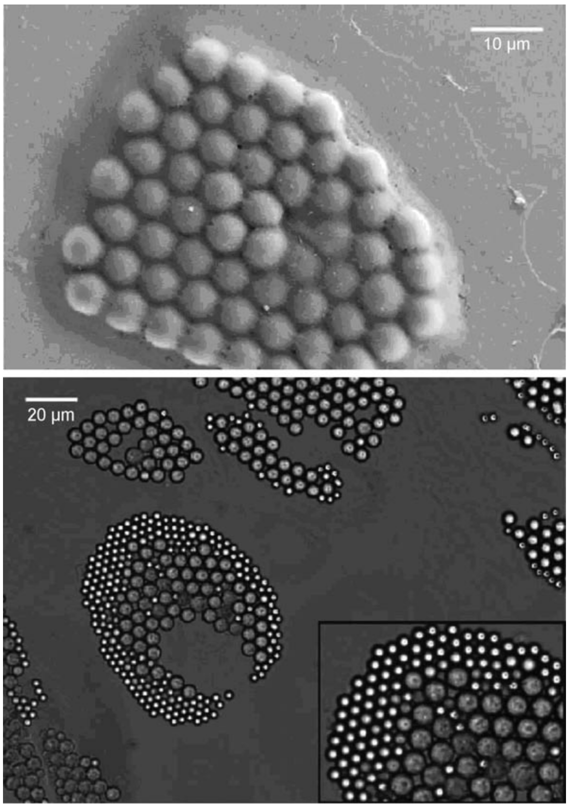

Figure 12. Top: Scanning electron micrograph of a fibroblast cell containing 6 μm PS particles organized into a hexagonal array. Bottom: Image showing size-dependent segregation of microspheres in fibroblast cells. Reproduced with permission from Reference [71], copyright 2007, the Royal Society of Chemistry.

3.7. Guiding Particle Assembly by External Fields

3.7.1. Light

Various approaches to guide the assembly of colloidal particles by light have been developed. These include both chemical and physical methods. One chemical approach was based on derivatizing both a substrate and colloidal silica particles with a photosensitive polymer containing spirobenzopyran photochromic molecules.[72] Exposure to $\lambda = 366$ nm light, induced ring-opening of the spirobenzopyran to the zwitterionic merocyanine form, whereas exposure to $\lambda = 585$ nm light reversed this process. Using these light-driven conversions, chemically distinct patterns with different polarity were generated by light exposure. The modified spheres adsorbed preferentially onto the merocyanine regions on the substrate. In a related approach, silica spheres were coated with a self-assembled monolayer of molecules that contained positively charged ammonium groups and *o*-nitrobenzene-protected carboxy groups, the protecting groups were cleaved upon light exposure to produce negatively charged carboxylate groups.[73] By varying the exposure time to UV light, the degree of cleavage could be changed, producing spheres with overall positive, neutral, or negative surface charges. As a result, the interactions between particles were modified.

Recently, an interesting new method has been developed to transport, trap, and sort colloids on planar substrates using low-intensity laser guidance. 2D surface plasmon excitations (collective oscillations of free electrons in an incident electromagnetic field) at metal–dielectric interfaces may be employed to guide colloidal particles under the influence of optical forces and optically induced, local, thermal-convection forces.[74] Using this technique, silica microspheres have been organized into hexagonally close-packed arrays and linear particle chains, depending on the power of the laser beam generating the optical interactions. Colloids can also be trapped at small metal patches on a patterned surface when optical forces overcome Brownian motion. The size dependence of such interactions has been used to guide particles size-selectively.[75]

Optical guidance of colloids is also possible by a different mechanism involving optoelectrofluidic control.[76,77] A colloidal suspension of charged PS spheres is placed between indium-tin-oxide-coated parallel plates, one of which contains a photoconductive layer. Optical image-driven dielectrophoresis permits high-resolution patterning of electric fields on the photoconductive substrate.[76] Upon light irradiation, the electric fields generated in the photoconductive layer bring about ion movement at the electric double layer. At certain frequencies, vortex regions and stagnant regions are produced. Colloidal crystallization occurs in the stagnant regions. The ratio of the distance between particles to their diameters increases as the applied alternating current (ac) frequency increases. By using this approach, array patterns consisting of lines and circles were achieved (Figure 13). It was also possible to dynamically merge and split circular shapes by the optoelectrofluidic mechanism.[77]

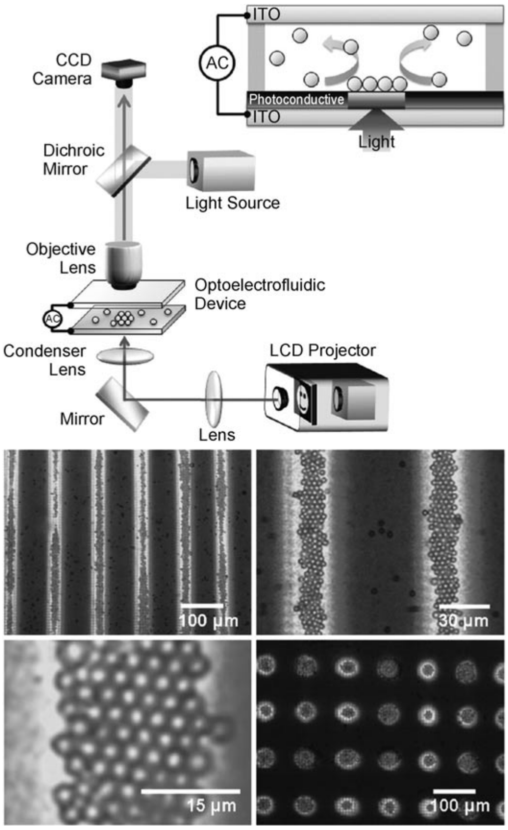

Figure 13. Top: Schematic diagram of the experimental setup for optoelectrofluidic assembly of colloids. AC = alternating current, CCD = charge coupled device, ITO = indium tin oxide. Bottom: Two-dimensional colloidal crystals fabricated using different image patterns. Reproduced with permission from Reference [77], copyright 2009, the American Chemical Society.

3.7.2. *Electric Fields*

Nucleation of colloidal crystals and growth of microwires assembled from colloidal particles can be induced by an alternating electric field between two electrodes on a surface.[78] Using such dielectrophoretic assembly, straight single microwires, multiply branched microwires, or parallel arrays of microwires were grown from 12–15 nm gold particles held together by van der Waals forces. These wires could be millimeters in length and micrometers in diameter. The assembled structures remained stable in the liquid matrix even after the electric field was turned off. If microwires broke while in the suspension, they self-repaired as more particles were attracted to the high intensity fields between electrode gaps. The growth patterns were influenced by multiple parameters, including the frequency, concentration of electrolyte, viscosity of the suspension, dielectric constant of the media, and gold-particle concentration in the suspension. For example, at lower frequency (ca. 100 Hz), assembly occurred mainly in the bulk, whereas at higher frequency (≥ 1000 Hz), surface assembly was predominant. A higher order of self-assembly beyond wire structures could be facilitated by using a biaxial electric field.[79] Alternatively, droplets containing colloidal particles can be manipulated by trapping them or transporting them with electric fields generated by addressable electrode arrays.[80]

3.7.3. *Magnetic Fields*

Paramagnetic colloidal particles can be readily guided by magnetic fields.[81] In the absence of an external magnetic field, spherical magnetic particles were observed to form linear chains.[82] On the other hand, in the presence of a magnetic field, spheres with magnetic caps assembled into syndiotactic chains, magnetic colloids with asymmetric dumbbell shapes into left-handed or right-handed helical chains, and colloids with symmetric dumbbell shapes assembled into chains with repeating in-plane/out-of-plane units.[82] Colloidal arrays with ring structures were produced by assembling a mixture of diamagnetic and paramagnetic spherical particles within a magnetized ferrofluid consisting of Fe_3O_4 nanoparticles suspended in water.[83] In this case, the mixtures of paramagnetic and diamagnetic particles interacted antiferromagnetically. The response of the particles depended on their magnetization relative to the ferrofluid. Particle arrays with a variety of shapes were obtained, including flowers, Saturn-like rings, and other multipolar structures. The assembly was self-limiting, resulting in large separations between individual structures rather than extensive crystallization. It should be noted that even nonmagnetic colloids can be guided by a magnetic field through a magnetic hole effect, if the colloids are immersed in a magnetic fluid.[84]

3.8. *Dynamic Self-Assembly*

Dynamic self-assembly may refer to several different concepts. Even within the scope of colloidal assembly research, the term has been used to describe very different systems. Broadly speaking, any self-assembly pattern requiring constant influx of energy can be categorized as dynamic self-assembly. According to Whitesides et al., a system undergoing dynamic self-assembly shall “*develop order only when dissipating energy*”.[85] The discussion in the following section will adopt a narrower definition[86] and only include self-assembly systems with at least one of the following features: assembly under a dynamic field, assembly through a dynamic process, or formation of a dynamic pattern.

One example of dynamic self-assembly occurs under a varying magnetic field. For example, paramagnetic PS spheres in suspension above a structured magnetic substrate line up along domain walls if the repeat distance of the ferromagnetic domains in the substrate is smaller than the colloid size.[87] Upon application of an oscillating magnetic field perpendicular to the film, particle arrays assemble or disassemble, depending on the amplitude of the imposed magnetic field modulation. Particles begin to move under the externally induced vibration of domain walls, following a 1D random walk perpendicular to the magnetic stripes, and organize into clusters at regions where the symmetry of the stripes is broken.

Dynamic self-assembly under the influence of a varying magnetic field has also been utilized to manipulate millimeter-sized PDMS disks doped with magnetite. Governed by a combination of a rotating magnetic field and interparticle repulsive forces, the magnetic disks formed a range of ordered patterns around the axial direction, where the symmetries depended on the disk size, rotating speed, and the number of disks.[85] In addition, when the magnetic disks had a chiral shape (e.g., the shape of comma), their interactions differed depending on the chirality, which could be further exploited to control the assembly, for example, into tail-to-tail structures.[88] Similar field-induced assembly of much smaller colloids has also been studied, at which length scale the van der Waals forces may become a prominent factor. Magnetic nickel particles approximately 100 μm in size exhibited snake-like patterns in a varying magnetic field,[89] which could be further complicated when colloids of a different size were introduced to break the symmetry and lead to directional self-propelling motion (Figure 14).[90] In a triaxial magnetic field, micrometer-sized superparamagnetic spheres exhibited an assembly path from dispersed colloids to branched bead strings and finally evolved into 2D ordered, self-healing patterns.[91] This phenomenon resembles biological self-assembly.[92]

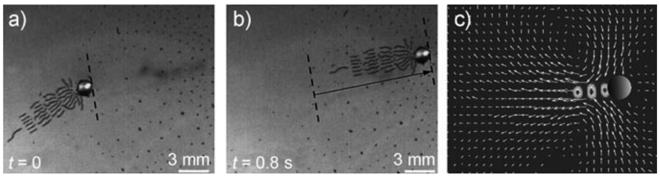

Figure 14. a), b) Asymmetric, snake-like colloidal chains in self-propelling motion under varying magnetic field. c) The corresponding velocity field map. Reproduced with permission from Reference [90], copyright 2009, the American Physical Society.

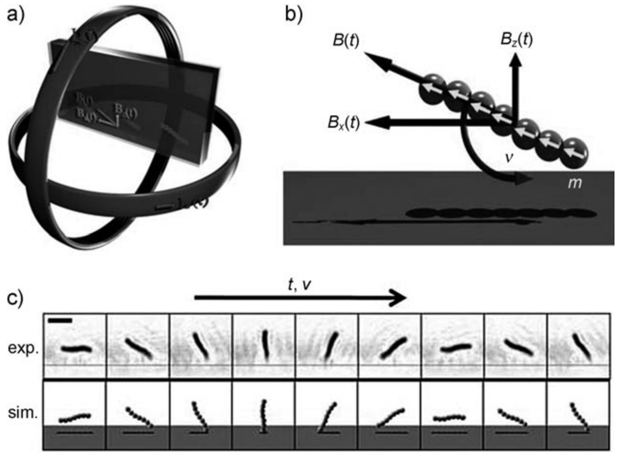

Figure 15. Self-assembly and motion of superparamagnetic colloidal chains ("surface walkers"). a) Illustration of the instrumental setup to control the magnetic field. b) Geometry of the "surface walker". c) Experimentally observed motion of the "surface walker" and corresponding simulation results, scale bar = 5 μm. Reproduced with permission from Reference [93], copyright 2010, the National Academy of Sciences of the USA.

Field-induced dynamic self-assembly is not necessarily limited to the interface. When a suspension of superparamagnetic colloids was subjected to a vertically rotating field (Figure 15 a), the magnetic colloidal chains moved according to the field dynamics (Figure 15 b) and behaved like rotors or so-called "surface walkers" (Figure 15 c).[93] In this study, the goal of self-assembly was not to achieve a definite colloidal structure. Instead, the focus was to develop a dynamic system by assembly. The rotation of in-situ assembled colloidal chains induced near-surface flow, which could be exploited for the transport of micro-objects. The velocity field created by the rotors was demonstrated to be capable of moving 20 μm vesicles.[93] In another study, the in-situ assembled colloidal clusters were used as valves for microfluidic devices.[94]

An intriguing idea is to realize complex colloidal assembly in a programmed manner. Inspired by DNA replication, a fundamental process for biological heredity, a road map was given to illustrate how colloidal self-replication may be realized in a similar fashion (Figure 16).[95] According to this scheme, the process starts with assembling a 'seed' colloidal bead string composed of, for example, two types of beads (A and B). The first step of the replication cycle is the 1:1 attachment of free A′ and B′ beads with the seed string, through complementary and reversible binding with A and B beads, respectively. Then the interactions between the A′ and B′ beads are activated, for example, through UV radiation, to form a string. In the last step, the initial A–A′ and B–B′ bonds are cleaved to release the replicated strings and allow the seed string to resume its original state for another replication cycle.[95] Although this fascinating approach is still under development, it nevertheless represents a very interesting direction.

4. Introducing Anisotropy and Directionality

To advance the analogy between syntheses of complex molecular structures and complex assemblies of colloids, it is necessary to endow particles with anisotropy and directionality.[96] For atoms and molecules this is facilitated by interactions between anisotropic orbitals. In the colloidal world, it requires either particles with anisotropic shapes or spherical colloids containing patches of another composition or site-specific functional groups pointing in different direc-

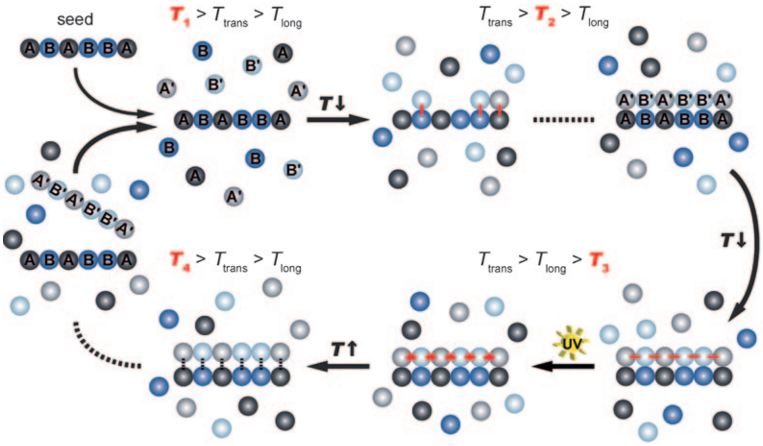

Figure 16. Illustration of the proposed DNA-mediated colloidal self-replication scheme. Single-stranded DNA surface groups on the permanently linked A and B particle chains direct the assembly of A′ and B′ particles with complementary DNA strands. Reproduced with permission from Reference [95], copyright 2009, the Royal Society of Chemistry.

tions. Although a wide selection of non-spherical colloids can be found, including platelets, cylinders, ellipsoids, rods, cubes, tetrahedra, star-shaped colloids, many studies to date are based on spherical building blocks that are combined or modified to lower the particle symmetry. Complex shapes have been achieved by stretching spherical polymer particles that are embedded in a flexible matrix,[97] deforming them by light irradiation or ion beam irradiation,[98] microfluidic synthesis,[99] controlled precipitation of sol–gel precursors in solution phase, and by various other methods that have been reviewed before.[68,100,101] Micro- and nanoparticles with at least two physically or chemically differing surfaces have been called "Janus particles" after De Gennes popularized this term nearly two decades ago.[102] Such particles may be considered as the materials equivalent of hydrophobin proteins in the biological world, that is, surface active proteins with both hydrophilic and hydrophobic patches.[103] They can provide dual functionality or act as surfactant-like particles if opposite faces have different surface polarity, surface charges, or surface functionalities. The definition of Janus particles has been further expanded to include spheres with different bulk composition in each hemisphere or spheres partially coated with other nanoparticles, capped on one side, or assembled with spheres of a different size.[104] As such, the asymmetry that allows directional binding can stem from both particle morphology and intrinsic asymmetry (e.g., charge, magnetic moment, and surface composition).[105]

4.1. Interfacial Methods

A common approach to breaking the symmetry of spheres is to deposit them on a substrate and then to modify the exposed surfaces toposelectively.[104] These may now be linked to another substrate to permit alteration of the opposite side, if desired.[106] For example, polymer spheres deposited on a substrate and coated on the top side with evaporated gold were subsequently modified with ionizable thiol groups on the gold patches to introduce pH-value-dependent electric dipoles on these spheres.[107] This treatment allowed the spheres to be aligned in an electric field or to induce electrophoretic rotation of the spheres with a pH-value-dependent response strength. Similarly, silica spheres were site-selectively patterned by e-beam spluttering of 1.0 nm Ti, then 2.5 nm Au. The Ti interlayer improved adhesion of the Au patches, which in turn permitted attachment of functional groups through thiol linkages.[108] The size of the gold patches could be altered by controlled etching after gold deposition, by annealing gold-coated silica spheres to form gold microcrystals on one side of each silica bead,[109] or by temporary masking of a part of the top surface before gold deposition. The last approach was exemplified by spin coating a thin layer of photoresist on the top surface of the spheres and then exposing a part of the spheres by plasma etching before gold deposition.[108] Discrete silica spheres with gold caps were obtained after dissolution of the photoresist and sonication. To add functionality to the opposite face, the gold patches were linked to a substrate using single-stranded DNA with thiol-derivatized end groups, followed by additional patterning of the new exposed surface. However, some spheres adsorbed to the surface with nonspecific orientation. Specificity could be partially improved by gentle sonication and multiple rinsing steps with buffer solutions.

Instead of using a photoresist mask, single or double overlayers of colloidal crystals can serve as masks during gold vapor deposition.[110] The pattern of the triangular interstices between spheres is then reproduced as gold patches on the spheres in the lowest layer, which can be isolated by peeling off the upper layers (Figure 17). Using this combination of

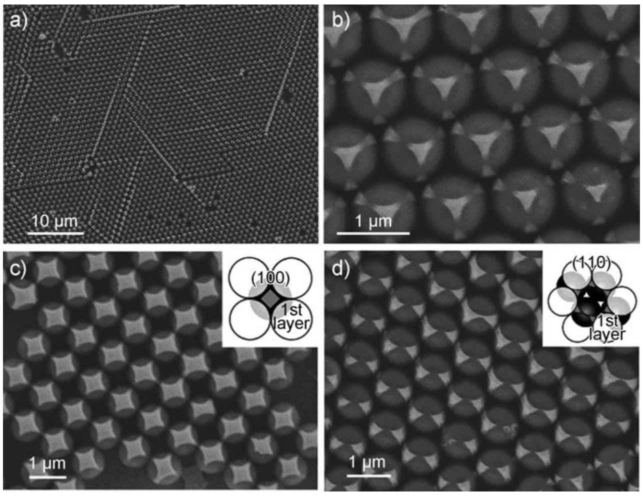

Figure 17. SEM images of gold-patterned PS spheres prepared by microsphere masking. a), b) Images of the patterns obtained with (111) facets of the colloidal crystals parallel to the substrate, c) with (100) faces, and d) with (110) faces parallel to the substrates. Reproduced with permission from Reference [110], copyright 2005, the American Chemical Society.

colloidal-crystal patterning with gold evaporation and plasma etching, spheres with 2–5 gold nanodots pointing in specific directions (linear, trigonal, tetrahedral, and square-based-pyramidal) can be obtained.[111] The dot pattern depends on both the layer level and the growth direction of the colloidal crystal.

As an alternative to modifying spheres on a solid substrate, sphere arrays may be placed at air–liquid or liquid–liquid interfaces to manipulate opposite hemispheres separately. As an example of the air–liquid approach, microspheres containing reactive ester groups were floated on water. Addition of NaOH to the aqueous phase resulted in removal of ester groups by hydrolysis, but only in the immersed region of the spheres. When the isolated spheres were exposed to human immunoglobulin G protein, the protein molecules were attached only to the hemisphere with the remaining reactive groups.[105] An example of asymmetric surface modification at a liquid–liquid interface involved PS spheres localized at a gel–hexane interface, replacing the hexane layer with PDMS and curing the PDMS left the particles partially embedded in the PDMS, the exposed surface could then be sputtered with a layer of gold.[112] The coated area could be controlled by adding surfactant to the aqueous gel phase, thereby altering the contact angle at the gel–hexane interface. Particles were mechanically removed from the PDMS matrix by scraping with a metal blade.

Spheres have also been modified asymmetrically by transferring a polymer monolayer onto one side of a supported sphere array using Langmuir–Blodgett techniques.[113] Unlike the previous techniques, this approach can be applied to nonreactive polymer spheres. Functionalized surface patches can then act as connecting points for further particle assembly.

Charge anisotropy was introduced by supporting charged spherical particles on a substrate and then printing water-insoluble ionic surfactants on the top surface of the supported particles using micro-contact printing with an elastomeric stamp.[114] This procedure introduced an electric dipole to the spherical particles. The extent of coverage was modulated by partially embedding the particles in a protective matrix. The particles formed short linear chains in the presence of salt solutions. Particle doublets and half-coated raspberry-like particles were formed by stamping the surfaces with particles of nearly comparable or much smaller size (quantum dots), respectively.

Arrays of snowman-like particles with interesting anti-reflective properties were grown on a planar substrate taking advantage of electrostatic interactions between interfaces.[115] First, PS particles with negative charge were attached to the substrate which had been coated with polyelectrolytes, terminating in a cationic layer. Next, the top surface of the PS spheres was coated with a polycationic ink by contact printing with a PDMS stamp. Smaller PS spheres with negative charge were then attached to the larger spheres, resulting in the snowman-like particles.

4.2. Confinement and Templating Methods

Asymmetric dimers of colloidal spheres of two different types (size, composition, etc.) can be prepared by combining geometrical confinement with sequential loading of two sets of spheres, followed by dewetting and annealing after each step. In an early example, a cell composed of two parallel glass slides was used, one slide being patterned with a 2D array of cylindrical holes in a photoresist.[116] The holes were first loaded with PS spheres whose diameter fell between the radius and the diameter of the holes, so that each hole contained only one PS sphere. After annealing the polymer spheres to fix them to the hole pattern, a silica-sphere suspension with spheres that could just fit in the remaining hole space was added, and solvent was allowed to evaporate. The resulting PS–silica dimers were stabilized by annealing and could be recovered by dissolving the photoresist.

A nanoporous membrane was used to direct the selective assembly of single citrate-stabilized gold nanoparticles[117] and nanoparticle chains[118] on larger silica spheres. The larger spheres were deposited on an ultrafiltration membrane filter with pores much smaller than the diameter of the particles. When gold nanoparticles were introduced from the opposite membrane side, they were trapped in the pores and some particles adsorbed to the surface of the amine-modified silica spheres (Figure 18).

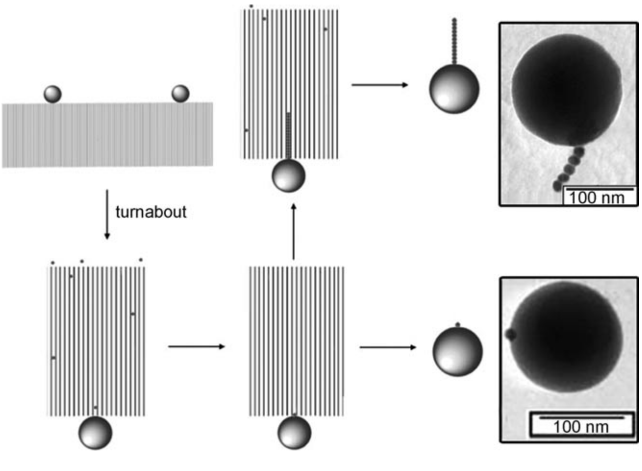

Figure 18. Assembly of gold nanoparticles on colloidal silica spheres by filtering the nanoparticles through a membrane. The microscopy images show silica spheres with one gold nanoparticle attached or with a gold nanoparticle chain. Reproduced with permission from Reference [118].

Colloidal-crystal templating is an effective and general approach to create shaped nanostructures with a wide range of materials.[31,119] This approach involves first the inverse replication of colloidal crystals into a 3DOM structure, followed by its disassembly into shaped building blocks (Figure 19). By this procedure, tetrapodal particles were obtained as dictated by the colloidal-crystal templates. The method was further developed to introduce site-selective functionalization to produce tip-tethered multipodal silica

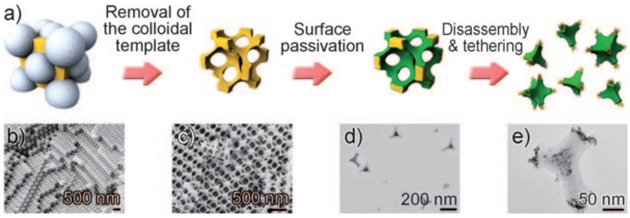

Figure 19. a) Synthesis of an end-tethered tetrapod based on colloidal crystal templating. SEM images of b) colloidal crystals and c) 3DOM silica. Transmission electron microscopy (TEM) images of d) tetrapodal silica particle after disassembly and e) gold NP adsorption on a tetrapod showing the site-specific functionalization. Reproduced with permission from Reference [120], copyright 2009, the American Chemical Society.

particles.[120] In this process, the surface of the 3DOM silica structure was first passivated with a dense layer of an organosilane. Then, following the disassembly of the 3DOM structure, the freshly generated (non-passivated) podal ends were selectively tethered with functional groups, such as thiols or amines, thereby granting them the capability of site-specific interactions. The distribution of surface functionality could be visualized by the adsorption of Au nanoparticles onto thiol tethered tetrapods (Figure 19).

4.3. Bulk Methods to Prepare Anisotropic Particles

Syntheses of non-spherical microspheres, dumbbells, and particles with raspberry surfaces by seeded polymerization methods are well documented.[121] Recently colloidal particles with the symmetry of water molecules were added to this collection.[122] Raspberry-like particles have also been prepared from polyelectrolyte multilayer-modified polymer particles.[123] The particles were dispersed in a solution of gold ions which adsorbed onto the amine groups of the polyelectrolytes and were reduced with $NaBH_4$. A silica shell was then added using a silicon alkoxide precursor. By treatment with KCN solution, the gold was leached out and the silica shell deformed to produce raspberry-like particles.

Instead of manipulating pre-formed colloids, it is possible to obtain Janus particles more directly. Biphasic colloids with two hemispheres differing in composition and/or surface functionality were produced by electrohydrodynamic jetting using side-by-side dual capillaries that provide two different liquid polymer precursors.[124] Modifying ligands, biomolecules, or fluorescing dyes could be incorporated in each precursor, as desired. By fragmenting the liquid jets, discrete biphasic and anisotropic particles were obtained. One disadvantage of this method was the relatively large size dispersity of the product particles, which would require an additional separation step when monodisperse particles are needed.

Significant progress has also been made in the anisotropic growth of semiconductor nanoparticles. Although most of these are smaller than the size range covered in this Review, a few examples will be provided, because they may serve as an inspiration for asymmetric modification of larger colloids, especially if these are crystalline. Anisotropy can be introduced through selective growth on the tips of colloidal semiconductor particles. Silver was grown on one end of ZnO nanorods by photoreduction of silver ions.[125] PbSe nanocrystals grew on one (CdS) or both tips (CdSe) of nanorods with wurtzite structure.[126] Tetrapodal structures are particularly interesting potential building blocks for three-dimensional superstructures. CdTe tetrapods can be fashioned with variable arm length from 20 to over 200 nm.[127] To prepare tetrapods with a single functionalized arm, CdTe tetrapods were deposited on a substrate, thereby breaking the tetrahedral symmetry of the nanoparticles. The three arms in contact with the substrate were passivated with a polymer layer by spin coating, leaving one arm for modification with thiol anchoring groups for gold nanoparticles. By breaking the gold-functionalized arms off the remaining structure, asymmetric nanorods were obtained.

Even when the primary building blocks are small, they may assemble into larger, anisotropic particles. ZnS clusters with uniform sizes and shapes were synthesized by a two-stage chemical precipitation process from metal salt and thioacetamide sulfide ion precursors.[128] The clusters were precipitated first at low temperature (26–32 °C) and then at higher temperature (85 °C). Spheres (500–3000 nm diameters) with low polydispersity and composed of 5–15 nm single-crystal spheroids were obtained, which clustered into micrometer-sized dimers, trimers, tetramers, and tetrahedra after the higher temperature treatment.

5. Stabilization/Consolidation of Assembled Colloidal Structures

The colloidal assemblies discussed in the previous sections, whether based on conventional or guided assembly, polarity, or interfacial interactions, do not involve strong chemical connections between colloids. In most instances, the adjacent colloids are merely in physical contact with each other, and the structures may not be robust enough to permit further handling. Hence an additional stabilization step is necessary, particularly for arresting colloidal structures in thermodynamically unstable or metastable states. The stabilization step may be incorporated in the assembly process. Alterations of the assembly process of micrometer-sized colloidal spheres into clusters by adding a secondary colloidal phase produced composite clusters. Such secondary components may consist of smaller particles that are deposited within the voids between larger colloids.[68] When a photocurable oil phase was added to such a reaction system, the resulting PS cluster structures produced in the oil-in-water emulsion could be stabilized after only a few seconds of exposure to UV light. Extraction of PS from the resin-stabilized spheres with toluene produced hollow clusters with open windows. The composite cluster approach also resulted in binary phases, and therefore surface anisotropy, when the photo-polymerized phase was doped with a fluorescent reagent.[101] Such cluster arresting could also take place in a single solvent. In a dispersion of Stöber silica colloids, dimer clusters could be formed through spontaneous attachment during colloid collisions by adjusting the colloid surface charge and the solvent polarity. Addition of fresh TEOS to the dispersion assisted the arresting of clusters by enabling a sol–gel reaction between the attached colloids.[129] In another approach, cross-linked PS or PMMA spheres were swelled with styrene monomer, and upon heat treatment, aspherical protrusions of the monomer droplets appeared on the swollen PS spheres (Figure 20a), whereas the monomer formed a uniform coating on the PMMA spheres (Figure 20b).[63] Therefore two different morphologies were obtained after the particles assembled into small clusters by coalescence. The clusters were subsequently stabilized by polymerizing the wetting layer.

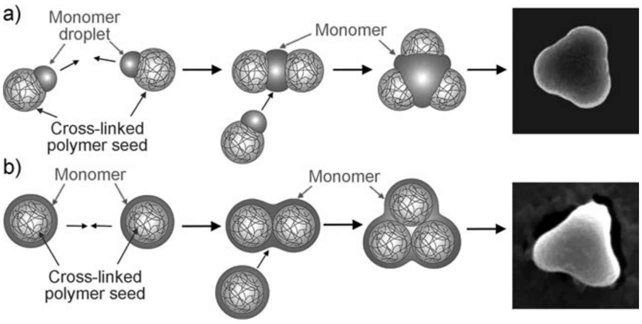

Figure 20. Colloidal clusters formed by a) liquid extrusion or b) wetting layers. Reproduced with permission from Reference [63], copyright 2009, the American Chemical Society.

Recently, a vapor-phase method was developed to arrest grouped colloids, in which a gaseous organosilica precursor was deposited to conjugate colloidal assemblies by capillary condensation.[130] In a capillary condensation process, reagent vapor preferentially condenses in confined spaces below its saturation vapor pressure and thus permits selective deposition of material in the vicinity of any contacting points between colloids. This approach was demonstrated to establish connections in colloidal clusters (Figure 21a) and 1D colloidal chains and would be easily adaptable to stabilize other self-assembled colloidal nanostructures. This simple method can be applied to a wide range of vaporizable materials, and it also permits conjugation of spatially separated particles. The capillary condensation was also used to modulate the surface functionality of colloidal structures (Figure 21b), as exemplified with tip-tethered tri-colloid clusters (Figure 21c,d), which are potentially capable of directional interactions and may be interesting building blocks for the self-assembly of open structures.

6. Connecting Particles

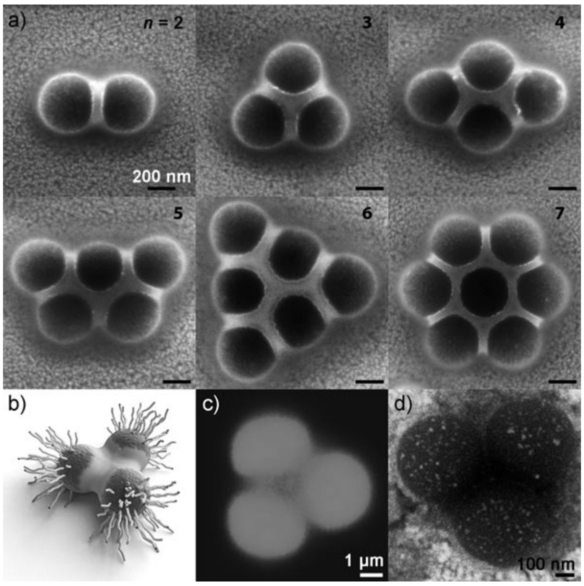

Figure 21. Conjugation and functionalization of colloidal clusters by capillary condensation. a) Conjugated clusters consisting of different number (*n*) of PS colloidal spheres. The white bands between the spheres are deposited organosilica. Scale bars all represent 200 nm. b) Schematic representation of a tip-tethered cluster. c) Confocal microscopy image of a fluorescent PS cluster after capillary condensation. d) Backscattered SEM image showing the adsorption of Au nanoparticles (white spots) on a conjugated, amine-functionalized PS cluster, where the Au spatial distribution is consistent with the confocal image in (c). Reproduced with permission from Reference [130], copyright 2009, the American Chemical Society.

Another approach to colloidal assembly involves modification of the colloid surface with appropriate functional groups. Short-range attractive forces at the molecular level, such as covalent bonds, dipolar interactions, hydrogen-bonding and donor–acceptor interactions can be readily applied to establish connections between colloids. However, since the length scale of these interactions is generally of molecular dimensions as well, ranging from a few Ångstroms up to nanometers, the interactions themselves are not sufficient to direct the assembly process of the colloids, and therefore additional assembly mechanisms need to be incorporated.

6.1. Direct/Complementary Bonding

When colloid surfaces are decorated with two complementary functional groups, spontaneous assembly can occur through their mutual binding. If the surface of the colloids is selectively functionalized, site-specific bonding can occur between colloids. A functional surface patch may be generated using various masking techniques. When dimer clusters formed by melamine formaldehyde colloids were settled in a Petri dish, smaller sulfated PS particles which were added to the dish spontaneously adsorbed on the cluster surfaces and masked out the surface amine groups on the colloids, except where the colloids were in contact with the substrate and with each other.[131] Thereafter, colloids with two amine patches were obtained, and they were able to bond with additional, much larger, sulfated PS colloids, resulting in water-molecule-like structures.[131]

Patches could also be formed on SiO_2 colloids with a masking layer on a substrate. A thin PMMA layer was applied to partially cover a monolayer of SiO_2 colloids, and then the remaining exposed area was subjected to surface functionalization. Subsequently, a secondary functionalization step could be undertaken on the covered area following the removal of PMMA. This strategy to generate Janus particles was verified by grafting two types of fluorescent agents to the particles and examining their spatial distribution, which confirmed the realization of surface anisotropy. In addition, by grafting with complementary coupling agents in a site-specific manner (Figure 22a,b), self-assembly through specific host–guest interactions into dimer clusters was demonstrated (Figure 22c).[132]

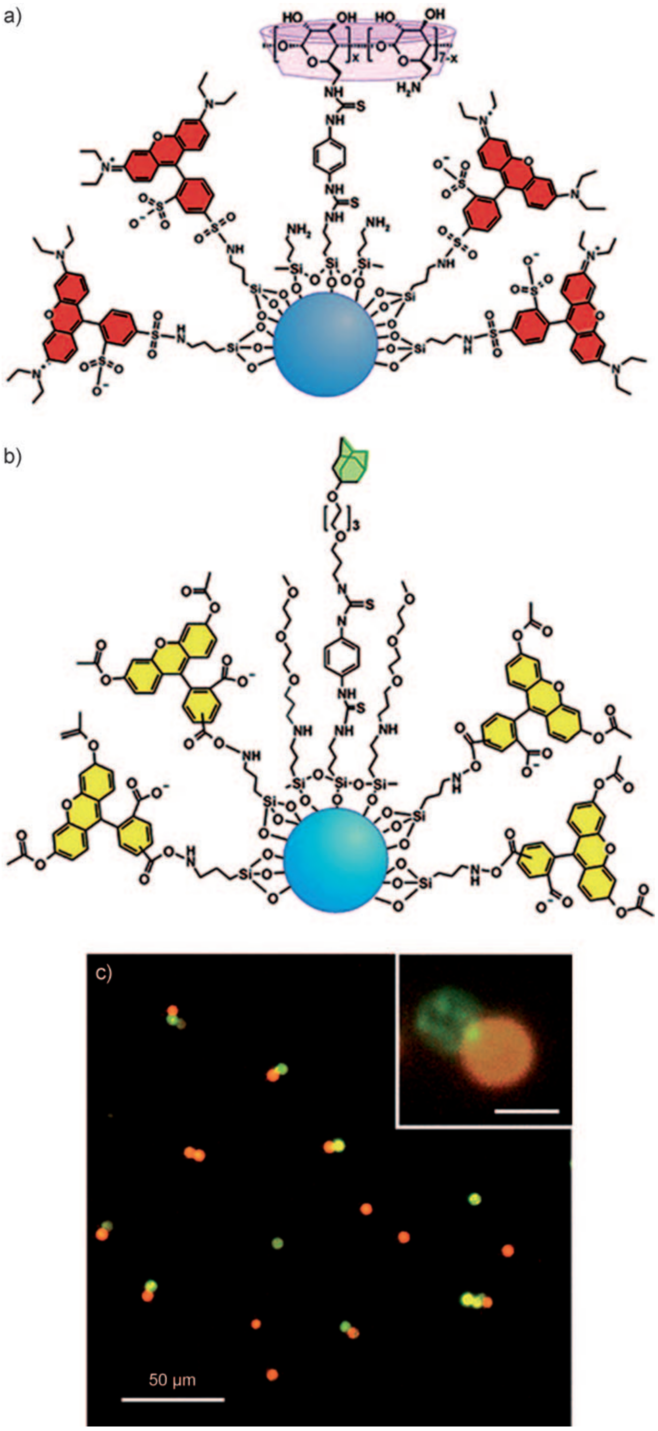

Figure 22. a), b) Janus particles with complimentary patches formed with masking techniques. The assembled dimer structures are shown in (c), Inset: scale bar 5 µm. Reproduced with permission from Reference [132].

6.2. Binding with Linkers (Coupling Agents)

Rather than involving colloids with complementary functional groups, the connection of a single type of functionalized colloids may be mediated by using a coupling agent or linker. A linker may simply connect two adjacent colloids, or with proper design, be able to bind multiple colloids and direct their final structures.[133] Recently, halogen bonding was explored for colloidal assembly. Halogen bonding refers to noncovalent interactions involving halogen aroms (except fluorine) as acceptors of electron density from Lewis bases. The tendency of halogen atoms to accept external electrons results from the anisotropy of electron density around halogen nuclei, which produces an electropositive crown along the colloid–halogen axis. Colloids, once functionalized with halogen donors, can engage in a self-assembly process by adding halogen-accepting linker molecules.[134] Essentially, halogen bonding is similar to hydrogen bonding, but it is considered to have higher strength. Therefore it may be suitable for connecting larger colloids.

The linkers may be extended from small molecules to include polymers. Structures assembled from colloids interacting with polymers may be described as "mortar-and-bricks" structures. Diaminotriazine-functionalized PS spheres and complementary thymine-functionalized gold colloids aggregate into clusters through three-point hydrogen-bonding interactions. The clusters consist of 3000–7000 individual nanoparticles per microsphere. The polymer acts as the "mortar" between gold "bricks" (Figure 23).[135] On the other hand, the mortar may also consist of very small nanoparticles. Amine-functionalized silica and carboxy-functionalized gold colloids were able to form mixed-colloid architectures.[136]

6.3. Linkage of Particles with Anisotropic Shapes

The connection of anisotropic particles through specific site-to-site interactions is highly desirable as it provides control over assembly behavior, opening doors for more complex structures that have been compared to molecular structures ("colloidal molecules"). When multiple interactions can be introduced these can lead to sequential assembly.[137] Metallic or semiconducting nanorods and multipods are excellent model systems to investigate anisotropic colloid assembly. Since these particles are typically formed through preferential growth of nanocrystals with amphiphilic molecules as stabilizers, it is possible to exploit dissimilar reactivities on different regions for selective functionalization. Biphasic rods and tetrapods were obtained through selective reduction of gold onto the tips of CdSe nanorods and tetrapods, where the crystalline surface was believed to be

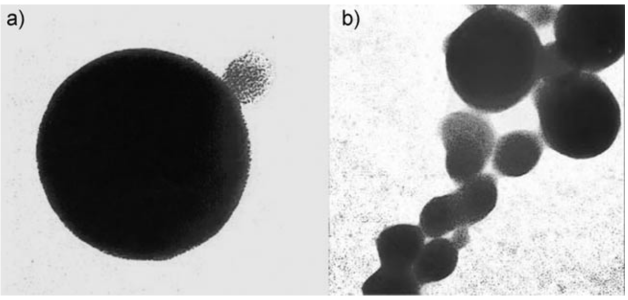

Figure 23. The self-assembly of gold nanoparticles and polymer into composite structures at different temperatures. a) at −20 °C and b) at 10 °C. Reproduced with permission from Reference [135], copyright 2000, Nature Publishing Group.

more reactive owing to increased surface energy and incomplete monolayer coverage.[138] Multiple particles could be tethered to each other using alkyl dithiol linkers between gold-functionalized tips, avoiding the more typical side-to-side assembly of rods.[138] Another way to induce the end-to-end assembly of the rods and tetrapods is promoted by controlling the solvent polarity.[139]

One recent study demonstrating the linking of particles in specific directions involves tethered silica tetrapods synthesized by colloidal crystals templating as described in Section 4.2.[120] The functionalized multipodal nanoparticles and colloidal silica spheres were used as building blocks to demonstrate the self-assembly of colloidal molecules. The tetrapodal particles were functionalized with triethoxysilylundecanal (Figure 24 a) to bind with approximately 45 nm in diameter aminated colloidal silica spheres (Figure 24 b) through reductive amination. As shown in Figure 24 c, silica colloids could be accurately mounted on the podal tips which have dimensions less than 20 nm. Meanwhile, no random adsorption on other regions was observed. With multiple colloidal silica spheres mounted onto one tetrapod, an ammonia-like-shaped colloidal molecule was formed (Figure 24 d–f). The precision of this assembly process demonstrates the advantage of assembly by anisotropic building blocks, and it may enable the fabrication of more complex, multi-component, functional assemblies in the future.

The selective functionalization on faceted colloids may also be achieved through a soft-lithography approach. Through selective functionalization of specific surfaces on silver nanocubes with a PDMS mold, definite assembly patterns were obtained which were dictated by the number of active facets (Figure 25).[140] When all the surfaces of the silver nanocubes were functionalized, a simple cubic array was obtained through assembly (Figure 25 f). It should be noted that such a particle array does not have any open space within the structure, which prevents its application as a photonic crystal. However, non-close-packed simple cubic arrays were realized through the natural assembly of composite cubes consisting of two types of materials, followed by selective etching in a controlled manner (Figure 26). In this case, if the “shells” of the particles are optically transparent, the “core” particles can be considered as non-close-packed simple cubic colloidal arrays.[141]

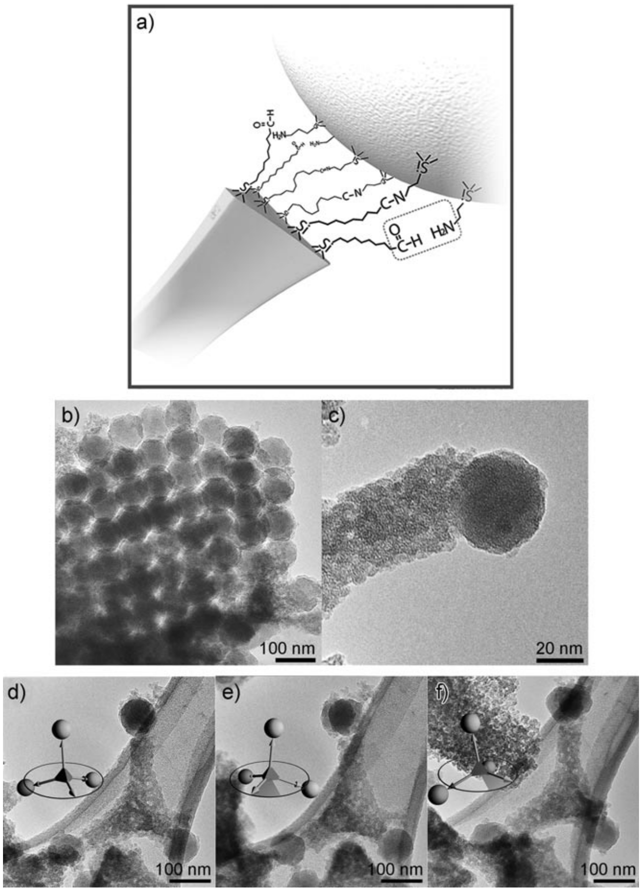

Figure 24. a) The directional assembly process based on reductive amination. b) Monodisperse silica colloidal spheres, approximately 45 nm in diameter, used in the assembly process. c) TEM image showing a silica colloid mounted on a podal end. d)–f) TEM images of different angles showing an ammonia-like nanostructure formed by three spherical silica colloids attached to one tetrapod. Reproduced with permission from Reference [120], copyright 2009, the American Chemical Society.

7. DNA-Directed Self-Assembly

One special type of hydrogen-bonding interaction is found between complementary DNA base pairs. Although individual hydrogen bonds may be relatively weak for colloidal assembly, the forces between complementary DNA strands can be quite strong due to the nature of the polyvalent interactions. Through direct grafting or interactions with certain chemical moieties, DNA oligomers can be introduced onto the colloidal surface. Connections are thus established by controlling DNA hybridization. DNA is widely used to link nanoparticles because it can be synthesized with specific lengths and sequences of functional groups that allow highly specific binding.[142] Since short-strand DNA or oligonucleotides with highly specific interactions can be synthesized in a programmable manner, DNA strands can be designed to bind strongly only with complementary strands. The binding and unbinding events, that is, the hybridization of complementary strands and the dissociation of the double-stranded helix are fully reversible and occur within a narrow temperature

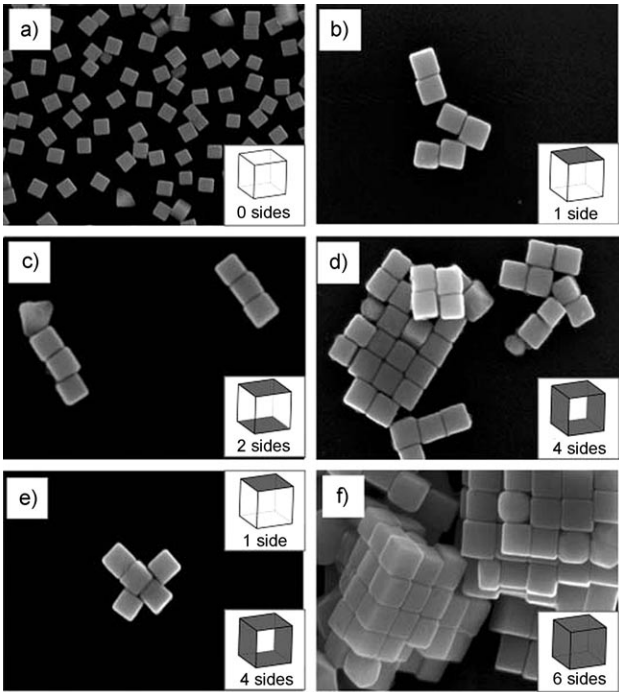

Figure 25. The self-assembly of silver nanocubes functionalized on selected surfaces (edge length ca. 100 nm). The number of functionalized surfaces is shown in each of the insets in a)–f). Reproduced with permission from Reference [140].

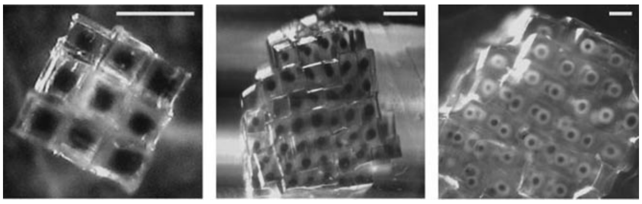

Figure 26. Three-dimensional array of sphere-in-cube particles prepared by selective etching of composite cubes. Scale bars = 1 mm. Reproduced with permission from Reference [141].

window called the melting temperature, thereby allowing modulation of the temperature to precisely control the magnitude of the attraction for self-assembly purposes. Typically, the designed DNA linkers have very low self-melt temperatures, making intrastrand loops and hairpin configurations unfavorable. However, purposely formed loops on the tails of the DNA linkers can serve for self-protection to provide better control over the assembly process.[143] The formation of internal hairpins inside DNA coatings occurs faster than interparticle binding, this improves the self-repair capability of assembly mistakes thus allowing more complex sequential assembly processes.[143]

Nanoparticle satellite structures were demonstrated by using gold particles of two different sizes decorated with complementary DNA strands.[144] In addition, if the colloid size ratios were carefully adjusted, the symmetry and coordination number could be controlled. A binary mixture of PS spheres with specific diameter ratios resulted in polyhedral clusters with ionic-crystal-like structures, including A_4B tetrahedral for $d_B/d_A \approx 0.23$ and A_6B octahedral for $d_B/d_A \approx 0.42$ (Figure 27).[145] On the other hand, the DNA linker could be programmed so that it could direct the final symmetry of the clusters. A pyramidal DNA linker was synthesized which allowed four colloidal particles to be attached on each corner. Using such a DNA linker as the scaffold, tetrapodal nanoparticle clusters were fabricated. In addition, chirality could be introduced by altering the DNA at the corners to control the sequential placement of different nanoparticles.[146]

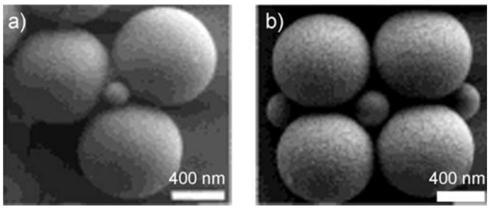

Figure 27. DNA based self-assembly of binary colloids into ordered structures. The small particles in the center of the images were surrounded by three (a) and four (b) large colloids, respectively. Reproduced with permission from Reference [145], copyright 2002, the American Chemical Society.

Another advantage of DNA linkers is that they offer flexible control of interparticle interactions. The extent of attractive interactions between DNA-functionalized PS spheres was varied by changing the hybridization segment length (a larger number of base-pair matches results in greater interaction), ionic strength (higher ionic strength results in stronger interactions as it reduces electrostatic repulsions), and composition of suspension mixtures.[147] In addition, the interaction energies between DNA-functionalized particles could be decreased by deliberately incorporating base-pair mismatches into the structure.[148] Reversible assembly of micro-sized colloids mediated by DNA was achieved by addition of a block-copolymer stabilizer, which provided suitable repulsion to prevent colloid arresting by van der Waals interactions.[149]

Further development of DNA-mediated assembly could benefit substantially from the introduction of anisotropy. Such anisotropy is achievable through appropriate design of the DNA tethers. By using a template DNA strand, multiple types of DNA tethers could be placed onto gold nanoparticles with precise control over their number and positions.[150] When a masking technique was combined with DNA hybridization, site-selective DNA attachment was realized.[151] Stable nanoparticle chains were formed by employing a combination of magnetic field effects to direct particle assembly and DNA interactions to stabilize the final structures.[152]

The ultimate goal and yet one of the biggest challenges for DNA-mediated assembly (and also for other colloidal assembly methods) is to realize self-assembly of highly ordered, extended structures. DNA hybridization has been used to create ordered 2D patterns of micrometer-sized colloids.[153] Meanwhile, control experiments showed that other methods employing biomolecules, such as biotin/avidin and carbodiimide, did not lead to ordered structures despite the fact that reversible aggregation could be achieved in these systems. This situation further underlined the importance of controlling the delicate interactions necessary for ordered assemblies. Recently, DNA modifications were successfully used to direct 3D ordered patterns, although with smaller gold nanoparticles.[154] The assembly was carried out at a temperature close to the melting point of DNA to allow reversible hybridization, as strong irreversible linkages typically produce irregular aggregates and prevent crystallization. The superlattice thus formed could be tuned through the DNA linkers.[155] Through studying the self-assembly process of DNA-bonded gold nanoparticles, several key steps in the process were clarified, especially the dependence of crystallization from an amorphous phase on the DNA components.[156]

An alternate approach is to assemble colloidal particles on a substrate. Thereafter, ordered structures may be achieved in a layer-by-layer manner.[157] In one example, a substrate was patterned by micro-contact printing with DNA. A monolayer of PS colloids with complimentary DNA was assembled on the patterned area through DNA hybridization and laser scattering was used as a facile approach to monitor the PS attachment.[158] However, in this case, the micro pattern was much larger than the colloids, which limited the spatial resolution. Controlled assembly with higher definition, preferably with single-particle precision, still remains a challenge, and yet this is an important next step in the development of substrate-assisted assembly.

8. Post-Assembly Issues

8.1. Removal of Surface Stabilizers

Colloids, especially small colloids, rely on surface protective layers for stabilization. However, in the final self-assembled structures, such surface layers introduce a significant fraction of organic material into the system. In a system of small colloidal particles, the amount of the organic species could be considerable and may lead to undesirable effects. Traditionally, the organic component is removed by calcination, which tends to destroy the nanometer-scale features as well. For example, nanocrystal quantum dots lose their luminescence after heating because unsaturated surface bonds resulting from ligand removal introduce trap states in the band gap.[159] Using a plasma treatment is an alternate method that offers several advantages over conventional heating.[160] In this technique, colloids are deposited on a substrate to form a thin film and are then treated with an air plasma. Surprisingly, the plasma induces polymerization of the ligand shell to form a polymer network, although upon completion the process leads to the removal of the entire organic phase. Therefore, through controlling the plasma process, a composite structure can be produced which offers improved chemical and mechanical stability. Recently, a unique Sn_2S_6 ligand was reported which could stabilize nanocrystals but was also capable of decomposing into a conductive SnS_2 phase upon brief heat treatment, while preserving the nanometer-scale nanocrystal features.[159]

8.2. Product Isolation and Purification

It is not uncommon that after assembly, the product contains both the desired assembly structures and unwanted side products. It therefore becomes necessary to find suitable approaches to isolate and sort the products from the mixture. Such processes may include gradient centrifugation and filtration. Gradient centrifugation allows separation of different objects based on their density or size, but it is generally a low-throughput process. In some processes, obtaining enough product through gradient centrifugation is a major bottleneck for scale-up.[161]

Alternatively, colloidal assemblies can be separated, sorted, focused, and driven through microchannels using diffusiophoresis, the movement of suspended colloidal particles under the influence of a gradient of a molecular solute. This process enhances migration of slowly diffusing colloids and provides better control over their transport. Diffusiophoresis can separate colloids carrying different surface charges, because these migrate at different rates.[162]

9. Theoretical Studies/Simulations

9.1. Challenges and Toolsets

The previous Sections discussed a wide range of different self-assembly processes governed by forces including van der Waals, electrostatic, hydrogen bonding, covalent, coordination, capillary, convective, shear, optical, and electromagnetic forces. It is the long-term expectation that, given sufficient understanding of these interactions, building blocks can be designed and manipulated to dictate the structure of the final product. Self-assembly of colloids by design, such as colloidal crystallization rather than amorphous gelation, requires control over both the magnitude and the length scale of the interactions.[163]

Although this Review focuses on colloids on the larger scale, typically above 50 nm, much can be learned from studies of self-assembly of smaller nanoparticles and clusters. However, several key differences need to be pointed out. Given the large particle size, bonding interactions (van der Waals, electrostatic, hydrogen bonding, and covalent bonding interactions) should be considered short-range forces that establish a connection only when the colloids are in very close proximity. They themselves cannot direct the assembly. On the other hand, these forces are strong enough to hinder separation of connected colloids, and therefore irreversible aggregation usually occurs before a thermodynamically stable state is reached. In addition, unlike small nanoparticles, the assembly of bigger colloids requires a large number of linkages. While under ideal conditions (atomic flatness), sufficient linkages are possible between adjacent surfaces, in real systems with significant surface roughness, the chances of forming effective interconnecting linkages become much smaller if interactions occur on the short range.[164] Another issue is the time scale. While molecular diffusion across a surface may only take seconds for 10 nm nanoparticles, it can take months for micron-sized colloids.[9] This time scale affects processes related to molecular diffusion (such as coalescence, surface modification and interparticle reactions) profoundly.[9]

Through theoretical studies, it can be concluded that properly designed colloids should result in the desired structure when equilibrium is reached and when the free energy of the system is minimal. Equally important, but much less predictable, is the kinetics of the assembly process. For example, one assembly pathway may lead to a stable state that is not necessarily the equilibrium state, or the time to achieve equilibrium may be too long and becomes impractical. The observed crystallization of a colloidal suspension proceeded by an initial nucleation process that was quite different from classical theory.[165] Therefore, a good understanding of the pathway to achieve the equilibrium configuration is also necessary to evaluate whether an assembly route is practically possible and to discover the most appropriate route.

9.2. Colloids with Isotropic Shape and Potential

Interactions of spheres with an isotropic potential had been widely studied even before the concept of colloidal self-assembly became popular. Spherical colloids, as the simplest model systems, mimic the thermodynamics of atomic crystals, providing a model for studying atomic crystallization. The atomic world demonstrates a very rich phase behavior through assembly, even when the potentials are simple. Therefore one direction of self-assembly by design towards highly ordered structures is through control of the form and range of the interaction potentials.

A critical stage of colloidal crystallization is the initial stage of nucleation. Despite the advancement of high-resolution TEM, which has started to permit direct observation of small crystalline clusters and even nucleation processes, much information is still experimentally inaccessible. Simulation is an effective tool to perceive phenomena that are beyond the capability of experimentation. In simulation it was found that small crystals formed but re-dissolved quickly unless they reached a critical size at which the high surface energy was balanced. Another important issue concerns the polydispersity of a colloidal system. A common rule of thumb is that highly crystalline phases are only attainable with less than 3% polydispersity. Simulation found that for 500 nm colloids, the crystallization could be completely suppressed with polydispersity greater than 10%, resulting in a completely amorphous phase.[166]

9.3. Isotropic Colloids in an External Field

Dipole–dipole interactions appear when an external field, typically an electrostatic or magnetic field, is applied to a colloidal dispersion. Experimentally, such external fields have been widely used to create 1D colloidal assemblies. The external field can also have a more fundamental impact on the assembly system, for example, by changing the ground state of the colloidal assembly. In a comprehensive simulation study, the phase diagram of both hard spheres (short-range repulsion) and soft spheres (long-range repulsion) was determined in an external electric or magnetic field. For hard spheres, the stable phases included face-centered cubic, hexagonal-close-packed, and body-centered-tetragonal phases. For the soft spheres an additional body-centered-orthorhombic phase was predicted.[167] These predictions agreed well with experimental studies in which the isotropic potential was tuned with ionic strength and an external electric field was applied to induce dipole–dipole interactions. The results confirmed the presence of these unusual phases and provided valuable insight into the assembly pathway (Figure 28).[168]

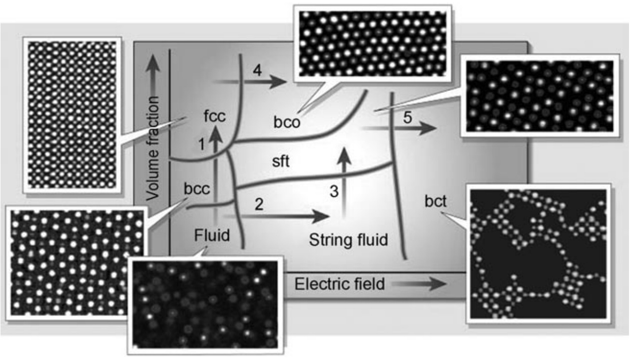

Figure 28. Phase diagram of a model colloid system under an electric field. Starting with a disordered fluid phase, an increase in volume fraction first leads to the formation of a body-centered cubic (bcc) phase, then to a face-centered cubic (fcc) phase (1). At higher electric fields, the disordered fluid phase converts into a string fluid (2), which transforms into a space-filling tetragonal (sft) phase upon an increase in volume fraction (3). At high volume fractions, an increase in electric field transforms the fcc phase into a body-centered orthorhombic (bco) phase (4) and the sft phase into a relatively open body-centered tetragonal (bct) phase. Reproduced with permission from Reference [86], copyright 2003, Nature Publishing Group.

Less explicit is the gravitational field. The effects of gravity can be gauged by the "scaled gravitational height" $h_{\mathrm{grav}}/2a$, where a is a scaling factor.[169] Roughly speaking, when this factor is close to unity, that is, the gravitational force is at the same level as thermal agitation, the effect of the gravitational field becomes prominent, and only when $h_{\mathrm{grav}}/2a \gg 1$ can the system be described as undergoing Brownian motion.[169]

9.4. Assembly of Amphiphilic Colloids (Janus Particles)

Amphiphilic colloids, such as Janus particles, are effective at imposing specific interparticle interactions, while remaining geometrically simple. Experimentally, various chain-like structures have been demonstrated by particles with such divalency.[170] Yet more complex structural control may be realized by developing a better understanding of these systems through simulation. It was shown by Monte Carlo simulations that spheres with oppositely charged hemispheres (zwitterionic Janus particles) can form clusters with definite shapes, in which the electric charge is distributed anisotropically (Figure 29).[171] Given the short-range of the electrostatic interactions compared with the sphere sizes, this model was found suitable to describe the self-assembly of weakly charged micron-sized colloidal spheres.[171] In a bigger model, a system containing 5000 zwitterionic Janus particles was sampled, and rich and unconventional phases were demonstrated. It was particularly noted that colloid clusters represent the stable phase over a rather wide range in the co-existence of individual particles (gas) and extended assembly (liquid).[172]

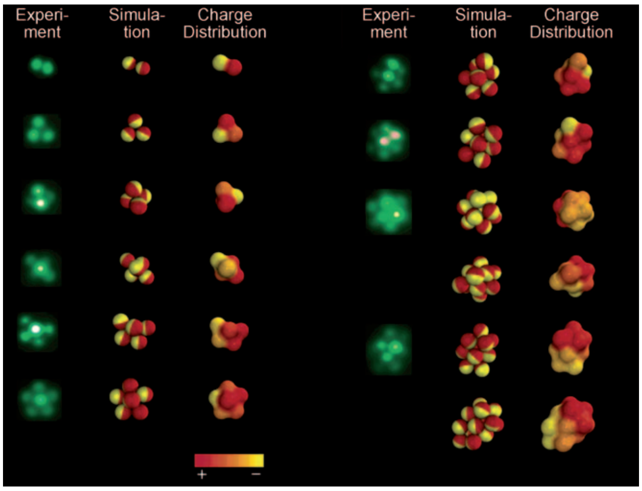

Figure 29. Experimental results and simulations of clusters formed by Janus colloids which have opposite charges on each hemisphere. Reproduced with permission from Reference [171], copyright 2006, the American Chemical Society.

9.5. Assembly of "Patchy" and Tethered Colloids

Just like in the molecular realm, colloids with "patchiness" (areas with different surface composition or properties) enable directional interactions between the active sites and lead to more precise control over assembly processes. As was shown in previous Sections, some of these general expectations have been demonstrated experimentally. Simulations with patchy models are expected to provide insight not only into nanoparticle self-assembly but also into other areas, such as protein crystallization and fluid dynamics. The modeling of patchy particles can be dated back to the 1980s, when similar research was conducted to investigate molecular structures.[173]

The stable phases formed by patchy colloids are functions of the pressure or volume fraction. As a simple case, the phase diagram of colloids with six patches in an octahedral configuration was computed, and the results showed that a simple cubic geometry is stable at low pressure but body-centered cubic and face-centered cubic arrays are preferred at high pressure.[174] The tendency to approach closer packing is in line with isotropic spheres. However, simulation also revealed that more fundamental changes could occur when the surface distribution of functional groups was altered, to the extent that the kinetics and thermodynamics of the assembly process needed to be re-examined. For particles with spherical potentials, the gas–liquid transition demanded a larger volume fraction of colloids when the particle–particle attraction decreased. The opposite trend appeared for patchy particles which exhibited directional interactions.[175]

Among the factors ruling the assembly of patchy colloids towards desired structures, the size of the patch is prominent.[176] A large patch size provides more flexibility and allows for more variety in possible assembly patterns, but smaller patches are necessary to avoid misassembly and ensure formation of the desired structures.[176,177]

Whereas with patches the functionality is limited to the near-colloid surface, tethers, while attached to the colloids, have at least one head group extending from the surface, which essentially creates a hybrid multi-element system. Patterns resembling those of surfactant assemblies were computed for colloids with single tethers.[178] More complex systems could be built from colloids with two different tethers. Governed by the tether directions and interactions, complex crystal structures were obtained, such as zinc blend, alternating tetragonal cylinders/tetragonal meshes, and alternating diamond structures.[179]

Low-density crystalline phases, or so-called open crystals, can be stabilized by anisotropic interactions. One intriguing goal for the assembly of patchy or tethered colloids is to realize the diamond structure, which provides a complete photonic band gap even at relatively low dielectric contrast, a highly coveted structure for photonic applications. The diamond structure would require the colloids to participate in strong directional interactions, as diamond structures found in nature result from tetrahedral covalent bonding. However, based on simulations, the situation turns out to be more complicated. In a comparative study, both six-patch (octahedral configuration) and four-patch (tetrahedral configuration) colloids were employed, aiming to reach crystalline structures. While the six-patch system was able to crystallize easily, leading to a perfect simple-cubic crystal, the four-patch system rarely showed any tendency for even partial crystallization (Figure 30).[180] In the four-patch system, the preferred local order overrode the global crystalline order and caused crystallization frustration.

Nevertheless, simulations also suggested several approaches to address this issue. Studies have shown that the presence of a small diamond seed could effectively induce further crystallization of the same configuration.[180,181] A recent simulation revealed that a seed may be created and recycled in the colloidal crystallization process.[182] An alternative strategy is based on the assembly of binary particles, such as oppositely charged tetrahedral colloids. This approach is different from a previous strategy for isotropic binary colloids, in which the formation of ionic crystal structures is controlled based on size differences.[183] Using oppositely charged particles, the aim is to manipulate the particle interaction,[184] which would penalize the formation of odd-

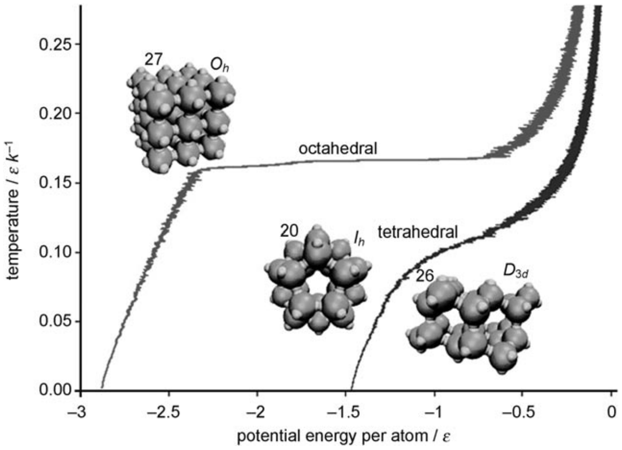

Figure 30. The potential-energy curves for cooling four-patch tetrahedral particles and six-patch octahedral particles. Insets: isolated clusters formed by four-patch and six-patch particles representing the global minimal energy states. Reproduced with permission from Reference [180], copyright 2007, the Royal Society of Chemistry.

numbered rings that existed in other structural motifs, thereby making the diamond structure more favorable.[180]

9.6. Non-Spherical Colloids

Shape can play an important role in colloidal assembly. Building blocks with non-spherical shapes offer different symmetries, packing densities, and directionalities and therefore, a greater variety of possible assembled structures is expected compared to their isotropic counterparts. As a result, classification of the particle morphology becomes more difficult. A conceptual framework was recently proposed as an attempt to put some order to the mixture of terminologies that has appeared in this multidisciplinary field of study. In this proposal, anisotropic particles were classified based on their 'dimensions', a composite parameter including the aspect ratio, faceting, surface pattern, branching, and roughness.[185]

Platonic solids probably represent the most basic and common structures for nanoparticulate materials. Geometrically these shaped particles offer different properties, such as symmetry, packing density, and anisotropy, that are of interest for studies ranging from materials to biological systems. The densest packing of a range of platonic solids has recently been described with the aid of a newly developed simulation method.[186] Another interesting area involves quasicrystal structures. Certain polyhedral colloids with symmetry properties forbidden in classical crystallography may potentially self-assemble into structures with long-range periodicity. The formation process, as suggested, involves kinetic trapping of building blocks into a growing nucleus with minimal rearrangement during solidification.[187] Such quasicrystal structures have many interesting properties, including significantly higher packing densities than crystalline phases and symmetries that are forbidden for crystalline structures.[188] A recent simulation revealed a range of beautiful quasicrystalline structures with high packing densities obtained from simple tetrahedra (Figure 31).[189]

Anisotropic particles can also be formed by grouping together a number of principle particles, such as various colloidal clusters formed by colloidal spheres. Asymmetric clusters may be formed by binding different colloids. A model system with cone-like particles was studied in which the particles were formed by a string of spheres. Such cone-shaped particles could spontaneously form clusters similar to colloidal clusters forming from colloidal spheres in an emulsion. In addition, more complex structures that were not yet available experimentally but are known to exist in biological systems were also observed.[190]

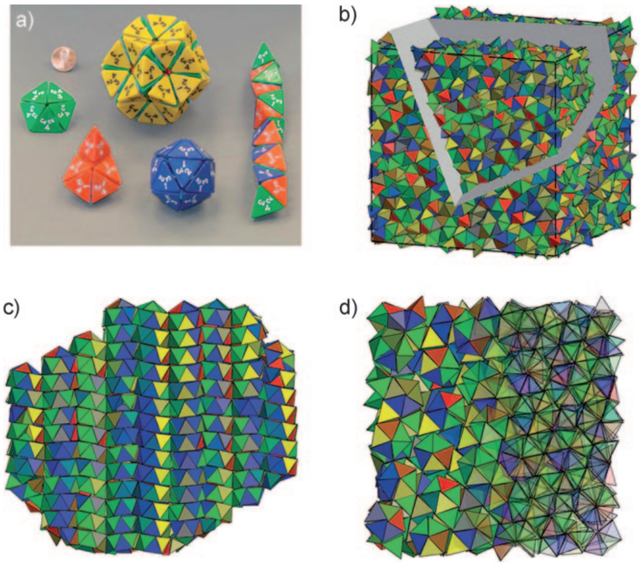

Figure 31. Tetrahedron packing a) by hand and b)–d) by simulations. Reproduced with permission from Reference [189], copyright 2009, Nature Publishing Group.

More complex colloids that have been synthesized are those having both structural and functional anisotropies. It is thus interesting to explore, theoretically, the possible assembly patterns and reveal structural correlations. The energy-minimization of such structures, however, was considered to be quite challenging because of the complicated interactions.[191] Tetris-like particles were investigated to evaluate their assembly on the basis of a two-dimensional square lattice.[192] When only nearest-neighbor interactions were considered, the computations predicted various stabilized aggregates where the arrangements depended on the building blocks and the clusters they formed (Figure 32).[191,192]

10. Applications of Colloidal Assembly

At this time, most of the applications of self-assembled colloids are based on 3D or 2D colloidal crystals, mainly exploiting their optical properties or their capabilities as templates for porous solids and membranes. An interesting trait of colloidal structures is related to their feature sizes,

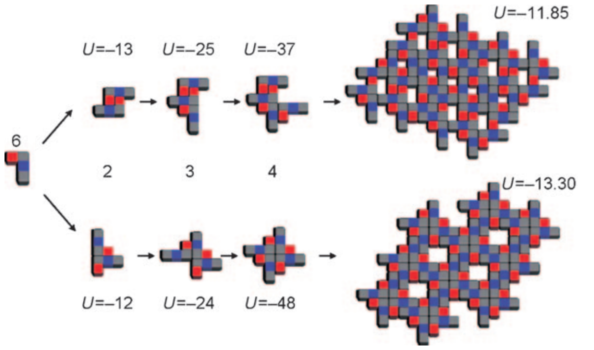

Figure 32. Examples of L-shaped "Tetris"-like building blocks (denoted as type "6" building blocks) into 2D periodic arrays. Different arrangements of dimers (2), trimers (3), tetramers (4), and larger clusters and their associated potential energies (*U*) are shown. Reproduced with permission from Reference [191], copyright 2009, the American Institute of Physics.

which are comparable to the wavelength of visible light. Opaline structures exhibit characteristic reflection spectra with so-called stop-bands, whose peak positions depend on the lattice spacing, refractive index contrast, and volume fractions of the components, as well as on the observation angle.[193] The associated colors are termed "structural colors", as they originate from interaction of light with the periodic structures and depend on the spacing of the structural features. Changes in transmission or reflection spectra and color result from infiltration of interstitial spaces with liquids, including liquid crystals whose refractive indices vary with temperature[194] and molecular orientation. Switching of optical states is possible by applying electric fields to opals infiltrated with liquid-crystal phases[195] or by filling the periodic arrays with photochromic dyes that can be switched reversibly by light irradiation.[196] Shifts in stop-band position as a function of temperature changes are possible by occluding ferroelectric components in the interstitial spaces.[197] Opaline structures composed of spherical colloids containing a superparamagnetic component exhibit colors that are highly responsive to magnetic fields.[198] These materials have been considered for use in reusable photonic paper whose color changes locally where the paper is infiltrated with a salt-based inking solution.[199]

Optical spectra of periodic sphere arrays are most responsive to changes in lattice spacing of the arrays. This change may be readily achieved by embedding colloidal particles in a swellable or stretchable matrix, such as hydrogels and elastomers. Composites of ordered silica spheres in hydrogel matrices have been demonstrated to function as optical sensors of temperature,[200] pH value,[201] ion concentration,[202] solvents,[203] certain analytes (e.g., glucose, creatinine),[204] and mechanical stresses.[205] By exchanging the water in a hydrogel matrix with photopolymerizable precursors, it is possible to generate and stabilize multicolor patterns in photonic-crystal hydrogels using appropriate photomasks.[206]

With silica spheres embedded in a redox-active metallopolymer, it was possible to create electrochromic and electromechanochromic composites, so called P-ink. These P-ink materials are suitable for constructing displays in which the initial colors are controlled by the fabrication process and can then be tuned by application of an electric potential.[207] Other suitable matrices for colloidal crystal-based displays include elastomers whose color responses vary with applied stresses.[208] Such systems have been tested in a biometric recognition device capable of forming images of fingerprints.[209] If solvents induce local swelling of the elastomer, the elastomer–sphere composites can be used as photonic papers.[210] Structural color may be fixed by arresting dynamically assembled, superparamagnetic colloids in a photopolymerized matrix. Based on this approach, coupled methods of magnetic color generation and photopolymerization were developed for printing patterns with high definition that mimick structural colors in nature (Figure 33).[211] Fabrication processes of elastomer composites containing soft polymer spheres were demonstrated to be suitable for scale-up, using extrusion and melt-flow techniques.[212] Deformable sheets were produced by these methods, and they displayed a range of different colors owing to differential deformation when placed into a hard, curved mold. The color intensity was further enhanced by incorporation of carbon nanoparticles in the polymer mixtures.[213]

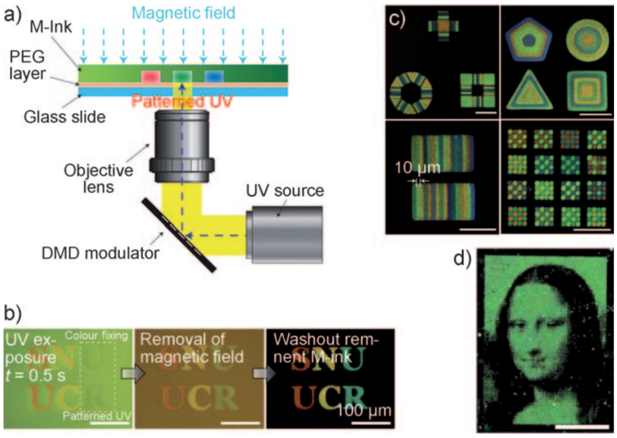

Figure 33. Structural color printing by magnetic-field-tuned assembly of superparamagnetic colloids. a) Illustration of color generation by adjusting magnetic field strength and color fixation by a photocurable polymer matrix; M-ink is a magnetic, photonic crystal based ink. b) An example of color generation and the fixation process. Patterned UV refers to patterned UV light reflected from a digital micromirror array modulator. scale bars = 100 µm. c) Different pattern formation and spatial definition; scale bars = 250 µm for the top left and bottom right image and 100 µm for the other two images. d) High-definition painting of the *Mona Lisa* based on structural color; scale bar = 2 mm. Reproduced with permission from Reference [211], copyright 2009, Nature Publishing Group.

Optical displays not based on photonic-crystal effects are also possible with a 2D assembly of Janus particles. An electric-field-driven display system was demonstrated by controlling the rotation of Janus spheres, in which each hemisphere was filled with black or white pigments, respectively.[214] A submonolayer coating of asymmetric colloidal clusters was found effective in anti-reflection coatings.[115] A

2D colloidal array was recently used to produce metamaterials for the visible and IR wavelength scales, which may eventually lead to the fabrication of usable optical nanocircuits.[215] 2D assembly of colloidal particles on a substrate also allows facile modification of the surface properties. A finely tuned colloidal layer could significantly alter the surface hydrophobicity to form a superhydrophobic surface.[42]

In addition, self-assembled colloidal structures can serve as templates for the fabrication of other functional materials. Polymer-coated magnetic colloid chains have been assembled to create carbon-particle chains after pyrolysis and magnetic-particle removal.[216] Colloidal-crystal templating is a relatively mature technique for the preparation of 3D porous structures.[217] When colloidal Janus particles coated with titania on one hemisphere were used for templating, the titania coating was transferred onto the surface of the porous replica for catalytic reactions.[218] Other potential applications that have been considered for colloidal structures prepared through self-assembly, include photonic/plasmonic devices, nanoscale electronics, high-efficiency energy conversion/storage, miniature diagnostic systems, drug/gene delivery, and hierarchically structured catalysts.[3,7]

11. Conclusions and Outlook

Successful assembly of colloidal particles into desirable structures depends on multiple parameters: 1) particle shapes and sizes, including size ratios in multimodal sets of particles; 2) the ability to balance repulsive and attractive interactions between particles and to orient anisotropic particles; and 3) interfacial and through-space interactions between particles and their surroundings. As illustrated by this Review, advances in synthesis and assembly of colloidal structures that address these parameters are progressing rapidly. The scope of colloidal assembly has been widened in recent years by the availability of new synthetic techniques to control colloid structures, compositions, surface properties, interactions, etc.

Particle morphologies are usually defined by crystal structure and specific growth parameters, but recent advancements in templating methods have provided the means for generating certain shapes independent of material composition and structure. Furthermore, progress in the synthesis of "colloidal molecules" provides new anisotropic building blocks that should be suitable for constructing progressively more complex colloidal oligomers, macromolecules, and crystals.

Management of particle–particle interactions has been simplified by methods of modifying colloid surfaces with functional groups that can vary charges as well as hydrophilicity and lipophilicity, both statically and dynamically. We have seen several examples where surface modifiers were applied only on small patches of the particles, sometimes with predefined directions to mimic multipolar features in the molecular regime. Advances in synthesizing particles that feature both desirable shapes and directional interactions are now setting the stage for the assembly of more complex structures. Carefully chosen materials and solvents are often necessary to provide a balanced system that avoids random aggregation of particles and, instead, brings them together in an organized fashion.

By employing methods for guiding assembly, as shown in this Review, it is possible to assemble colloidal structures that do not represent the most thermodynamically stable arrangements. If these can be locked into place by forming strong interactions, it becomes possible to achieve molecular analogues of kinetically stabilized structures, including very open structures that have been elusive for colloidal assemblies. Guidance through spatial confinement or by interfaces provides the means for attaining unusual geometries and patterns. Currently, such patterns are often first generated by top-down approaches that limit their resolution. However, ongoing improvements in resolution are starting to blur the gap between top-down and bottom-up methods, so that these may be used in conjunction.[219] Similar technological improvements also apply to the resolution of external forces employed to guide particles. The examples of using external forces (magnetic fields, light, etc.) reviewed herein typically applied to 2D structures. Another big step forward can be expected if new techniques of particle manipulation are developed to assemble colloids in 3D arrays with a spatial precision that matches that of holograms.

Simulations have given much insight into assembly processes and interactions, at times making bold but often, accurate predictions of attainable structures and assembly routes. They are providing a basis for further experimental exploration.

Scale-up of methods to afford larger yields of building blocks and assembled materials will be important for commercialization of "designed" colloidal assemblies,[7] but we can still expect many improvements on the smaller scale to enhance the assortment of building blocks and assembled structures. It is possible to imagine a structure composed of separate colloidal building blocks, each providing specific functionality and perhaps interacting synergistically with the functionality of the overall structure. Proposals for colloidal arrays to produce optical metamaterials are the first step towards complex functionality, such as optical nanocircuits.[215] Applications of colloidal structures, though still in their infancy, hold great promise for the future.

We gratefully acknowledge support by the National Science Foundation (DMR-0704312) and by the US Department of Energy (DE-FG02-06ER46348) Parts of our work were carried out in the Institute of Technology Characterization Facility, University of Minnesota, which receives partial support from the NSF through the NNIN and MRSEC programs.

Received: March 10, 2010

---

[1] V. J. Anderson, H. N. W. Lekkerkerker, *Nature* **2002**, *416*, 811; U. Gasser, *J. Phys. Condens. Matter* **2009**, *21*, 203101.
[2] H. Zhang, E. W. Edwards, D. Wang, H. Möhwald, *Phys. Chem. Chem. Phys.* **2006**, *8*, 3288.

[3] G. A. Ozin, K. Hou, B. V. Lotsch, L. Cademartiri, D. P. Puzzo, F. Scotognella, A. Ghadimi, J. Thomson, *Mater. Today* **2009**, *12*, 12.

[4] E. Matijević, *Acc. Chem. Res.* **1981**, *14*, 22.

[5] S. John, *Phys. Rev. Lett.* **1987**, *58*, 2486; J. D. Joannopoulos, R. D. Meade, J. N. Winn, *Photonic Crystals*, Princeton Univ. Press, Princeton, **1995**.

[6] Y. Xia, B. Gates, Y. Yin, Y. Lu, *Adv. Mater.* **2000**, *12*, 693.

[7] O. D. Velev, S. Gupta, *Adv. Mater.* **2009**, *21*, 1897.

[8] M. P. Pileni, *Acc. Chem. Res.* **2008**, *41*, 1799.

[9] Y. Min, M. Akbulut, K. Kristiansen, Y. Golan, J. Israelachvili, *Nat. Mater.* **2008**, *7*, 527.

[10] E. C. Nelson, P. V. Braun, *Science* **2007**, *318*, 924.

[11] Y. K. Koh, C. H. Yip, Y.-M. Chiang, C. C. Wong, *Langmuir* **2008**, *24*, 5245; F. Marlow, Muldarisnur, P. Sharifi, R. Brinkmann, C. Mendive, *Angew. Chem.* **2009**, *121*, 6328; *Angew. Chem. Int. Ed.* **2009**, *48*, 6212.

[12] P. D. Kaplan, J. L. Rouke, A. G. Yodh, D. J. Pine, *Phys. Rev. Lett.* **1994**, *72*, 582.

[13] J. K. G. Dhont, C. Smits, H. N. W. Lekkerkerker, *J. Colloid Interface Sci.* **1992**, *152*, 386.

[14] L. V. Woodcock, *Nature* **1997**, *385*, 141.

[15] N. D. Denkov, O. D. Velev, P. A. Kralchevsky, I. B. Ivanov, H. Yoshimura, K. Nagayama, *Nature* **1993**, *361*, 26; P. Jiang, J. F. Bertone, K. S. Hwang, V. L. Colvin, *Chem. Mater.* **1999**, *11*, 2132; H. Cong, W. Cao, *Langmuir* **2003**, *19*, 8177.

[16] S. H. Im, Y. T. Lim, D. J. Suh, O. O. Park, *Adv. Mater.* **2002**, *14*, 1367.

[17] T. Kanai, T. Sawada, *Langmuir* **2009**, *25*, 13315.

[18] L. Wang, X. S. Zhao, *J. Phys. Chem. C* **2007**, *111*, 8538.

[19] J. V. Sanders, M. J. Murray, *Nature* **1978**, *275*, 201.

[20] S. Hachisu, S. Yoshimura, *Nature* **1980**, *283*, 188; P. Bartlett, R. H. Ottewill, P. N. Pusey, *Phys. Rev. Lett.* **1992**, *68*, 3801; N. Hunt, R. Jardine, P. Bartlett, *Phys. Rev. E* **2000**, *62*, 900; V. Kitaev, G. A. Ozin, *Adv. Mater.* **2003**, *15*, 75; H. Cong, W. Cao, *J. Phys. Chem. B* **2005**, *109*, 1695.

[21] L. Wang, Y. Wan, Y. Li, Z. Cai, H.-L. Li, X. S. Zhao, Q. Li, *Langmuir* **2009**, *25*, 6753.

[22] Z. Zhou, Q. Yan, Q. Li, X. S. Zhao, *Langmuir* **2007**, *23*, 1473.

[23] A. Rugge, S. H. Tolbert, *Langmuir* **2002**, *18*, 7057.

[24] M. E. Leunissen, C. G. Christova, A.-P. Hynninen, C. P. Royall, A. I. Campbell, A. Imhof, M. Dijkstra, R. van Roij, A. van Blaaderen, *Nature* **2005**, *437*, 235.

[25] E. C. M. Vermolen, A. Kujik, L. C. Filion, M. Hermes, J. H. J. Thijssen, M. Dijkstra, A. van Blaaderen, *Proc. Natl. Acad. Sci. USA* **2009**, *106*, 16063.

[26] P. Bartlett, A. I. Campbell, *Phys. Rev. Lett.* **2005**, *95*, 128302.

[27] A. M. Kalsin, M. Fialkowski, M. Paszewski, S. K. Smoukov, K. J. M. Bishop, B. A. Grzybowski, *Science* **2006**, *312*, 420.

[28] E. V. Shevchenko, D. V. Talapin, N. A. Kotov, S. O'Brien, C. B. Murray, *Nature* **2006**, *439*, 55; E. V. Shevchenko, D. V. Talapin, C. B. Murray, S. O'Brien, *J. Am. Chem. Soc.* **2006**, *128*, 3620.

[29] T. Ming, X. Kou, H. Chen, T. Wang, H.-L. Tam, K.-W. Cheah, J.-Y. Chen, J. Wang, *Angew. Chem.* **2008**, *120*, 9831; *Angew. Chem. Int. Ed.* **2008**, *47*, 9685.

[30] B. Pietrobon, M. McEachran, V. Kitaev, *ACS Nano* **2009**, *3*, 21.

[31] F. Li, Z. Wang, A. Stein, *Angew. Chem.* **2007**, *119*, 1917; *Angew. Chem. Int. Ed.* **2007**, *46*, 1885.

[32] F. Li, S. A. Delo, A. Stein, *Angew. Chem.* **2007**, *119*, 6786; *Angew. Chem. Int. Ed.* **2007**, *46*, 6666.

[33] E. P. Lewandowski, J. A. Bernate, A. Tseng, P. C. Searson, K. J. Strebe, *Soft Matter* **2009**, *5*, 886.

[34] F. Li, Y. Qian, A. Stein, *Chem. Mater.* **2010**, *22*, 3226.

[35] F. Garcia-Santamaría, H. T. Miyazaki, A. Urquía, M. Ibisate, M. Belmonte, N. Shinya, F. Meseguer, C. López, *Adv. Mater.* **2002**, *14*, 1144.

[36] A. van Blaaderen, R. Ruel, P. Wiltzius, *Nature* **1997**, *385*, 321; K.-H. Lin, J. C. Crocker, V. Prasad, A. Schofield, D. A. Weitz, T. C. Lubensky, A. G. Yodh, *Phys. Rev. Lett.* **2000**, *85*, 1770.

[37] G. A. Ozin, S. M. Yang, *Adv. Funct. Mater.* **2001**, *11*, 95; Y. Yin, L. Yu, B. Gates, Y. Xia, *J. Am. Chem. Soc.* **2001**, *123*, 8718; S. M. Yang, H. Míguez, G. A. Ozin, *Adv. Funct. Mater.* **2002**, *12*, 425; Y. Xia, Y. Yin, Y. Lu, J. McLellan, *Adv. Funct. Mater.* **2003**, *13*, 907.

[38] Y. Yin, Y. Xia, *J. Am. Chem. Soc.* **2003**, *125*, 2048.

[39] R. E. Schaak, R. E. Cable, B. M. Leonard, B. C. Norris, *Langmuir* **2004**, *20*, 7293.

[40] M. Rycenga, P. H. C. Camargo, Y. Xia, *Soft Matter* **2009**, *5*, 1129.

[41] N. N. Khanh, K. B. Yoon, *J. Am. Chem. Soc.* **2009**, *131*, 14228.

[42] G. Zhang, D. Wang, Z.-Z. Gu, H. Möhwald, *Langmuir* **2005**, *21*, 9143.

[43] H. Zheng, M. F. Rubner, P. T. Hammond, *Langmuir* **2002**, *18*, 4505.

[44] J. Aizenberg, P. V. Braun, P. Wiltzius, *Phys. Rev. Lett.* **2000**, *84*, 2997.

[45] W. M. Choi, O. O. Park, *Colloids Surf. A* **2006**, *277*, 131.

[46] A. R. Tao, J. Huang, P. Yang, *Acc. Chem. Res.* **2008**, *41*, 1662.

[47] J. Huang, F. Kim, A. R. Tao, S. Connor, P. Yang, *Nat. Mater.* **2005**, *4*, 896.

[48] J. Huang, A. R. Tao, S. Connor, R. He, P. Yang, *Nano Lett.* **2006**, *6*, 524.

[49] S. Acharya, J. P. Hill, K. Ariga, *Adv. Mater.* **2009**, *21*, 2959.

[50] S. C. Warren, F. J. Disalvo, U. Wiesner, *Nat. Mater.* **2007**, *6*, 156.

[51] K. P. Sharma, G. Kumaraswamy, I. Ly, O. Mondain-Monval, *J. Phys. Chem. B* **2009**, *113*, 3423.

[52] M. Fukao, A. Sugawara, A. Shimojima, W. Fan, M. A. Arunagirinathan, M. Tsapatsis, M. Okubo, *J. Am. Chem. Soc.* **2009**, *131*, 16344.

[53] M. S. Nikolic, C. Olsson, A. Salcher, A. Kornowski, A. Rank, R. Schubert, A. Frömsdorf, H. Weller, S. Förster, *Angew. Chem.* **2009**, *121*, 2790; *Angew. Chem. Int. Ed.* **2009**, *48*, 2752.

[54] L. Carbone, L. Manna, C. Sönnichsen, *Angew. Chem.* **2009**, *121*, 4346; *Angew. Chem. Int. Ed.* **2009**, *48*, 4282.

[55] T. M. Hermans, M. A. C. Broeren, N. Gomopoulos, P. van der Schoot, M. H. P. van Genderen, N. A. J. M. Sommerdijk, G. Fytas, E. W. Meijer, *Nat. Nanotechnol.* **2009**, *4*, 721.

[56] D. R. Nelson, *Nano Lett.* **2002**, *2*, 1125.

[57] I. Muševič, M. Škarabot, U. Tkalec, M. Ravnik, S. Žumer, *Science* **2006**, *313*, 954.

[58] U. Ognysta, A. Nych, V. Nazarenko, I. Muševič, M. Škarabot, M. Ravnik, S. Žumer, I. Poberaj, D. Babič, *Phys. Rev. Lett.* **2008**, *100*, 217803.

[59] U. Ognysta, A. Nych, V. Nazarenko, M. Škarabot, I. Muševič, *Langmuir* **2009**, *25*, 12092.

[60] C. P. Lapointe, T. G. Mason, I. I. Smalyukh, *Science* **2009**, *326*, 1083.

[61] A. D. Dinsmore, M. F. Hsu, M. G. Nikolaides, M. Marquez, A. R. Bausch, D. A. Weitz, *Science* **2002**, *298*, 1006.

[62] J.-W. Kim, A. Fernández-Nieves, N. Dan, A. S. Utada, M. Marquez, D. A. Weitz, *Nano Lett.* **2007**, *7*, 2876.

[63] D. J. Kraft, W. S. Vlug, C. M. van Kats, A. van Blaaderen, A. Imhof, W. K. Kegel, *J. Am. Chem. Soc.* **2009**, *131*, 1182.

[64] G.-R. Yi, T. Thorsen, V. N. Manoharan, M.-J. Hwang, S.-J. Jeon, D. J. Pine, S. R. Quake, S.-M. Yang, *Adv. Mater.* **2003**, *15*, 1300; Z. Nie, S. Xu, M. Seo, P. C. Lewis, E. Kumacheva, *J. Am. Chem. Soc.* **2005**, *127*, 8058.

[65] J.-I. Park, Z. Nie, A. Kumachev, A. I. Abdelrahman, B. P. Binks, H. A. Stone, E. Kumacheva, *Angew. Chem.* **2009**, *121*, 5404; *Angew. Chem. Int. Ed.* **2009**, *48*, 5300.

[66] V. N. Manoharan, M. T. Elsesser, D. J. Pine, *Science* **2003**, *301*, 483; V. N. Manoharan, *Solid State Commun.* **2006**, *139*, 557.

[67] D. Zerrouki, B. Rotenberg, S. Abramson, J. Baudry, C. Goubault, F. Leal-Calderon, D. J. Pine, J. Bibette, *Langmuir* **2006**, *22*, 57; S. Korkut, D. A. Saville, I. A. Aksay, *Langmuir* **2008**, *24*, 12196.
[68] S.-Y. Cho, G.-R. Yi, J.-M. Lim, S.-H. Kim, V. N. Manoharan, D. J. Pine, S.-M. Yang, *J. Am. Chem. Soc.* **2005**, *127*, 15968.
[69] F. Li, X. Badel, J. Linnros, J. B. Wiley, *J. Am. Chem. Soc.* **2005**, *127*, 3268; M. Tymczenko, L. F. Marsal, T. Trifonov, I. Rodriguez, F. Ramiro-Manzano, J. Pallares, A. Rodriguez, R. Alcubilla, F. Meseguer, *Adv. Mater.* **2008**, *20*, 2315.
[70] J.-M. Lim, J. H. Moon, G.-R. Yi, C.-J. Heo, S.-M. Yang, *Langmuir* **2006**, *22*, 3445.
[71] V. K. Kodali, W. Roos, J. P. Spatz, J. E. Curtis, *Soft Matter* **2007**, *3*, 337.
[72] M. Piech, M. C. George, N. S. Bell, P. V. Braun, *Langmuir* **2006**, *22*, 1379.
[73] K. N. Plunkett, A. Mohraz, R. T. Haasch, J. A. Lewis, J. S. Moore, *J. Am. Chem. Soc.* **2005**, *127*, 14574.
[74] V. Garcés-Chávez, R. Quidant, P. J. Reece, G. Badenes, L. Torner, K. Dholakia, *Phys. Rev. B* **2006**, *73*, 085417.
[75] M. Righini, A. S. Zelenina, C. Girard, R. Quidant, *Nat. Phys.* **2007**, *3*, 477.
[76] P. Y. Chiou, A. T. Ohta, M. C. Wu, *Nature* **2005**, *436*, 370.
[77] H. Hwang, Y.-H. Park, J.-K. Park, *Langmuir* **2009**, *25*, 6010.
[78] K. D. Hermanson, S. O. Lumsdon, J. P. Williams, E. W. Kaler, O. D. Velev, *Science* **2001**, *294*, 1082; K. H. Bhatt, O. D. Velev, *Langmuir* **2004**, *20*, 467; K.-Q. Zhang, X. Y. Liu, *Nature* **2004**, *429*, 739.
[79] M. E. Leunissen, H. R. Vutukuri, A. van Blaaderen, *Adv. Mater.* **2009**, *21*, 3116.
[80] J. R. Millman, K. H. Bhatt, B. G. Prevo, O. D. Velev, *Nat. Mater.* **2005**, *4*, 98.
[81] J. Ge, Y. Yin, *J. Mater. Chem.* **2008**, *18*, 5041.
[82] D. Zerrouki, J. Baudry, D. Pine, P. Chaikin, J. Bibette, *Nature* **2008**, *455*, 380.
[83] R. M. Erb, H. S. Son, B. Samanta, V. M. Rotello, B. B. Yellen, *Nature* **2009**, *457*, 999.
[84] A. T. Skjeltorp, *Phys. Rev. Lett.* **1983**, *51*, 2306.
[85] B. A. Grzybowski, H. A. Stone, G. M. Whitesides, *Nature* **2000**, *405*, 1033.
[86] W. B. Russell, *Nature* **2003**, *421*, 490.
[87] P. Tierno, T. M. Fischer, T. H. Johansen, F. Sagués, *Phys. Rev. Lett.* **2008**, *100*, 148304.
[88] B. A. Grzybowski, G. M. Whitesides, *Science* **2002**, *296*, 718.
[89] A. Snezhko, I. S. Aranson, W. K. Kwok, *Phys. Rev. Lett.* **2006**, *96*, 078701; M. Belkin, A. Snezhko, I. S. Aranson, W. K. Kwok, *Phys. Rev. Lett.* **2009**, *102*, 158301.
[90] A. Snezhko, M. Belkin, I. S. Aranson, W. K. Kwok, *Phys. Rev. Lett.* **2009**, *102*, 118103.
[91] N. Osterman, I. Poberaj, J. Dobnikar, D. Frenkel, P. Ziherl, D. Babic, *Phys. Rev. Lett.* **2009**, *103*, 228301.
[92] J. F. Douglas, *Nature* **2010**, *463*, 302.
[93] C. E. Sing, L. Schmid, M. F. Schneider, T. Franke, A. Alexander-Katz, *Proc. Natl. Acad. Sci. USA* **2010**, *107*, 535.
[94] T. Sawetzki, S. Rahmouni, C. Bechinger, D. W. M. Marr, *Proc. Natl. Acad. Sci. USA* **2008**, *105*, 20141.
[95] M. E. Leunissen, R. Dreyfus, R. Sha, T. Wang, N. C. Seeman, D. J. Pine, P. M. Chaikin, *Soft Matter* **2009**, *5*, 2422.
[96] Z. Mao, H. Xu, D. Wang, *Adv. Funct. Mater.* **2010**, *20*, 1053.
[97] T. Ding, Z.-F. Liu, K. Song, K. Clays, C.-H. Tung, *Langmuir* **2009**, *25*, 10218.
[98] E. Snoeks, A. van Blaaderen, T. van Dillen, C. M. van Kats, M. L. Brongersma, A. Polman, *Adv. Mater.* **2000**, *12*, 1511; E. Snoeks, A. van Blaaderen, T. van Dillen, C. M. van Kats, M. L. Velikov, M. L. Brongersma, A. Polman, *Nucl. Instrum. Methods Phys. Res. Sect. B* **2001**, *178*, 62.
[99] D. Dendukuri, K. Tsoi, T. A. Hatton, P. S. Doyle, *Langmuir* **2005**, *21*, 2113; D. Dendukuri, D. C. Pregibon, J. Collins, T. A. Hatton, P. S. Doyle, *Nat. Mater.* **2006**, *5*, 365.
[100] Y. Lu, Y. Yin, Y. Xia, *Adv. Mater.* **2001**, *13*, 415.
[101] S.-H. Kim, G.-R. Yi, K.-H. Kim, S.-M. Yang, *Langmuir* **2008**, *24*, 2365.
[102] P. G. de Gennes, *Rev. Mod. Phys.* **1992**, *64*, 645.
[103] A. Walther, A. H. E. Müller, *Soft Matter* **2008**, *4*, 663.
[104] A. Perro, S. Reculusa, S. Ravaine, E. Bourgeat-Lami, E. Duguet, *J. Mater. Chem.* **2005**, *15*, 3745.
[105] K. Fujimoto, K. Nakahama, M. Shidara, H. Kawaguchi, *Langmuir* **1999**, *15*, 4630.
[106] S. Jiang, S. Granick, *Langmuir* **2009**, *25*, 8915.
[107] H. Takei, N. Shimizu, *Langmuir* **1997**, *13*, 1865.
[108] Z. Bao, L. Chen, M. Weldon, E. Chandross, O. Cherniavskaya, Y. Dai, J. B.-H. Tok, *Chem. Mater.* **2002**, *14*, 24.
[109] Y. Lu, H. Xiong, X. Jiang, Y. Xia, M. Prentiss, G. M. Whitesides, *J. Am. Chem. Soc.* **2003**, *125*, 12724.
[110] G. Zhang, D. Wang, H. Moehwald, *Nano Lett.* **2005**, *5*, 143.
[111] G. Zhang, D. Wang, H. Möhwald, *Angew. Chem.* **2005**, *117*, 7945; *Angew. Chem. Int. Ed.* **2005**, *44*, 7767.
[112] V. N. Paunov, O. J. Cayre, *Adv. Mater.* **2004**, *16*, 788.
[113] K. Nakahama, H. Kawaguchi, K. Fujimoto, *Langmuir* **2000**, *16*, 7882.
[114] O. Cayre, V. N. Paunov, O. D. Velev, *J. Mater. Chem.* **2003**, *13*, 2445.
[115] H. Y. Koo, D. K. Yi, S. J. Yoo, D.-Y. Kim, *Adv. Mater.* **2004**, *16*, 274.
[116] Y. Yin, Y. Lu, Y. Xia, *J. Am. Chem. Soc.* **2001**, *123*, 771.
[117] L. Nagle, D. Ryan, S. Cobbe, D. Fitzmaurice, *Nano Lett.* **2003**, *3*, 51.
[118] L. Nagle, D. Fitzmaurice, *Adv. Mater.* **2003**, *15*, 933.
[119] A. Stein, F. Li, Z. Wang, *J. Mater. Chem.* **2009**, *19*, 2102.
[120] F. Li, W. C. Yoo, M. B. Beernink, A. Stein, *J. Am. Chem. Soc.* **2009**, *131*, 18548.
[121] K. Furusawa, Y. Kimura, T. Tagawa, *J. Colloid Interface Sci.* **1986**, *109*, 69; A. T. Skjeltorp, J. Ugelstad, T. Ellingsen, *J. Colloid Interface Sci.* **1986**, *113*, 577; M. Okubo, K. Kanaida, T. Matsumoto, *Colloid Polym. Sci.* **1987**, *265*, 876; H. R. Sheu, M. S. El-Aasser, J. W. Vanderhoff, *J. Polym. Sci. Part A* **1990**, *28*, 653; J.-E. Joensson, H. Hassander, L. H. Jansson, B. Törnell, *Macromolecules* **1991**, *24*, 126; S. Reculusa, C. Poncet-Legrand, S. Ravaine, C. Mingotaud, E. Duguet, E. Bourgeat-Lami, *Chem. Mater.* **2002**, *14*, 2354; S. Reculusa, C. Poncet-Legrand, A. Perro, E. Duguet, E. Bourgeat-Lami, C. Mingotaud, S. Ravaine, *Chem. Mater.* **2005**, *17*, 3338.
[122] J.-G. Park, J. D. Forster, E. R. Dufresne, *Langmuir* **2009**, *25*, 8903.
[123] W. S. Choi, H. Y. Koo, W. T. S. Huck, *J. Mater. Chem.* **2007**, *17*, 4943.
[124] K.-H. Roh, D. C. Martin, J. Lahann, *Nat. Mater.* **2005**, *4*, 759.
[125] C. Pacholski, A. Kornowski, H. Weller, *Angew. Chem.* **2004**, *116*, 4878; *Angew. Chem. Int. Ed.* **2004**, *43*, 4774.
[126] S. Kudera, L. Carbone, M. F. Casula, R. Cingolani, A. Falqui, E. Snoeck, W. J. Parak, L. Manna, *Nano Lett.* **2005**, *5*, 445.
[127] H. Liu, A. P. Alivisatos, *Nano Lett.* **2004**, *4*, 2397.
[128] C. M. Liddell, C. J. Summers, *Adv. Mater.* **2003**, *15*, 1715.
[129] M. Ibisate, Z. Zou, Y. Xia, *Adv. Funct. Mater.* **2006**, *16*, 1627.
[130] F. Li, A. Stein, *J. Am. Chem. Soc.* **2009**, *131*, 9920.
[131] C. E. Snyder, M. Ong, D. Velegol, *Soft Matter* **2009**, *5*, 1263.
[132] X. Y. Ling, I. Y. Phang, C. Acikgoz, M. D. Yilmaz, M. A. Hempenius, G. J. Vancso, J. Huskens, *Angew. Chem.* **2009**, *121*, 7813; *Angew. Chem. Int. Ed.* **2009**, *48*, 7677.
[133] M. A. Olson, A. Coskun, R. Klajn, L. Fang, S. K. Dey, K. P. Browne, B. A. Grzybowski, J. F. Stoddart, *Nano Lett.* **2009**, *9*, 3185.

[134] T. Shirman, T. Arad, M. E. van der Boom, *Angew. Chem.* **2010**, *122*, 938; *Angew. Chem. Int. Ed.* **2010**, *49*, 926.

[135] A. K. Boal, F. Ilhan, J. E. DeRouchey, T. Thurn-Albrecht, T. P. Russell, V. M. Rotello, *Nature* **2000**, *404*, 746.

[136] T. H. Galow, A. K. Boal, V. M. Rotello, *Adv. Mater.* **2000**, *12*, 576.

[137] H. Onoe, K. Matsumoto, I. Shimoyama, *Small* **2007**, *3*, 1383.

[138] T. Mokari, E. Rothenberg, I. Popov, R. Costi, U. Banin, *Science* **2004**, *304*, 1787.

[139] A. Figuerola, I. R. Franchini, A. Fiore, R. Mastria, A. Falqui, G. Bertoni, S. Bals, G. Van Tendello, S. Kudera, R. Cingolani, L. Manna, *Adv. Mater.* **2009**, *21*, 550.

[140] M. Rycenga, J. M. McLellan, Y. Xia, *Adv. Mater.* **2008**, *20*, 2416.

[141] P. J. Wesson, S. Soh, R. Klajn, K. J. M. Bishop, T. P. Gray, B. A. Grzybowski, *Adv. Mater.* **2009**, *21*, 1911.

[142] A. P. Alivisatos, K. P. Johnsson, X. Peng, T. E. Wilson, C. J. Loweth, M. P. Bruchez, Jr., P. G. Schultz, *Nature* **1996**, *382*, 609; C. A. Mirkin, R. L. Letsinger, R. C. Mucic, J. J. Storhoff, *Nature* **1996**, *382*, 607.

[143] M. E. Leunissen, R. Dreyfus, F. C. Cheong, D. G. Grier, R. Sha, N. C. Seeman, P. M. Chaikin, *Nat. Mater.* **2009**, *8*, 590.

[144] R. C. Mucic, J. J. Storhoff, C. A. Mirkin, R. L. Letsinger, *J. Am. Chem. Soc.* **1998**, *120*, 12674.

[145] C. M. Soto, A. Srinivasan, B. R. Ratna, *J. Am. Chem. Soc.* **2002**, *124*, 8508.

[146] A. J. Mastroianni, S. A. Claridge, A. P. Alivisatos, *J. Am. Chem. Soc.* **2009**, *131*, 8455.

[147] V. T. Milam, A. L. Hiddessen, J. C. Crocker, D. J. Graves, D. A. Hammer, *Langmuir* **2003**, *19*, 10317.

[148] A. J. Kim, R. Scarlett, P. L. Biancaniello, T. Sinno, J. C. Crocker, *Nat. Mater.* **2009**, *8*, 52.

[149] M. P. Valignat, O. Theodoly, J. C. Crocker, W. B. Russel, P. M. Chaikin, *Proc. Natl. Acad. Sci. USA* **2005**, *102*, 4225.

[150] K. Suzuki, K. Hosokawa, M. Maeda, *J. Am. Chem. Soc.* **2009**, *131*, 7518.

[151] M. M. Maye, D. Nykypanchuk, M. Cuisinier, D. van der Lelie, O. Gang, *Nat. Mater.* **2009**, *8*, 388.

[152] D. Li, J. Rogers, S. L. Biswal, *Langmuir* **2009**, *25*, 8944.

[153] A. J. Kim, P. L. Biancaniello, J. C. Crocker, *Langmuir* **2006**, *22*, 1991; P. L. Biancaniello, A. J. Kim, J. C. Crocker, *Phys. Rev. Lett.* **2005**, *94*, 058302.

[154] S. Y. Park, A. K. R. Lytton-Jean, B. Lee, S. Weigand, G. C. Schatz, C. A. Mirkin, *Nature* **2008**, *451*, 553; D. Nykypanchuk, M. M. Maye, D. van der Lelie, O. Gang, *Nature* **2008**, *451*, 549.

[155] H. D. Hill, R. J. Macfarlane, A. J. Senesi, B. Lee, S. Y. Park, C. A. Mirkin, *Nano Lett.* **2008**, *8*, 2341.

[156] R. J. Macfarlane, B. Lee, H. D. Hill, A. J. Senesi, S. Seifert, C. A. Mirkin, *Proc. Natl. Acad. Sci. USA* **2009**, *106*, 10493.

[157] B. Kannan, R. P. Kulkarni, A. Majumdar, *Nano Lett.* **2004**, *4*, 1521.

[158] M. H. S. Shyr, D. P. Wernette, P. Wiltzius, Y. Lu, P. V. Braun, *J. Am. Chem. Soc.* **2008**, *130*, 8234.

[159] M. V. Kovalenko, M. Scheele, D. V. Talapin, *Science* **2009**, *324*, 1417.

[160] L. Cademartiri, A. Ghadimi, G. A. Ozin, *Acc. Chem. Res.* **2008**, *41*, 1820.

[161] H. A. Jerri, W. P. Sheehan, C. E. Snyder, D. Velegol, *Langmuir* **2010**, *26*, 4724.

[162] B. Abécassis, C. Cottin-Bizonne, C. Ybert, A. Ajdari, L. Bocquet, *New J. Phys.* **2009**, *11*, 075022.

[163] K. J. M. Bishop, C. E. Wilmer, S. Soh, B. A. Grzybowski, *Small* **2009**, *5*, 1600.

[164] A. Kulak, Y. S. Park, Y. J. Lee, Y. S. Chun, K. Ha, K. B. Yoon, *J. Am. Chem. Soc.* **2000**, *122*, 9308.

[165] U. Gasser, E. R. Weeks, A. Schofield, P. N. Pusey, D. A. Weitz, *Science* **2001**, *292*, 258.

[166] S. Auer, D. Frenkel, *Nature* **2001**, *413*, 711.

[167] A.-P. Hynninen, M. Dijkstra, *Phys. Rev. Lett.* **2005**, *94*, 138303.

[168] A. Yethiraj, A. van Blaaderen, *Nature* **2003**, *421*, 513.

[169] A. Yethiraj, *Soft Matter* **2007**, *3*, 1099.

[170] S. K. Smoukov, S. Gangwal, M. Marquez, O. D. Velev, *Soft Matter* **2009**, *5*, 1285.

[171] L. Hong, A. Cacciuto, E. Luijten, S. Granick, *Nano Lett.* **2006**, *6*, 2510.

[172] F. Sciortino, A. Giacometti, G. Pastore, *Phys. Rev. Lett.* **2009**, *103*, 237801.

[173] J. Kolafa, I. Nezbeda, *Mol. Phys.* **1987**, *61*, 161.

[174] E. G. Noya, C. Vega, J. P. K. Doye, A. A. Louis, *J. Chem. Phys.* **2007**, *127*, 054501.

[175] E. Bianchi, J. Largo, P. Tartaglia, E. Zaccarelli, F. Sciortino, *Phys. Rev. Lett.* **2006**, *97*, 168301.

[176] A. W. Wilber, J. P. K. Doye, A. A. Louis, *J. Chem. Phys.* **2009**, *131*, 175101.

[177] R. Fantoni, D. Gazzillo, A. Giacometti, M. A. Miller, G. Pastore, *J. Chem. Phys.* **2008**, *127*, 234507.

[178] Z. Zhang, M. A. Horsch, M. H. Lamm, S. C. Glotzer, *Nano Lett.* **2003**, *3*, 1341.

[179] C. R. Iacovella, S. C. Glotzer, *Nano Lett.* **2009**, *9*, 1206.

[180] J. P. K. Doye, A. A. Louis, I. C. Lin, L. R. Allen, E. G. Noya, A. W. Wilber, H. C. Kok, R. Lyus, *Phys. Chem. Chem. Phys.* **2007**, *9*, 2197.

[181] Z. Zhang, A. S. Keys, T. Chen, S. C. Glotzer, *Langmuir* **2005**, *21*, 11547.

[182] A. Cacciuto, S. Auer, D. Frenkel, *Nature* **2004**, *428*, 404.

[183] A.-P. Hynninen, J. H. J. Thijssen, E. C. M. Vermolen, M. Dijkstra, A. van Blaaderen, *Nat. Mater.* **2007**, *6*, 202.

[184] C. G. Sztrum, E. Rabani, *Adv. Mater.* **2006**, *18*, 565.

[185] S. C. Glotzer, M. J. Solomon, *Nat. Mater.* **2007**, *6*, 557.

[186] S. Torquato, Y. Jiao, *Nature* **2009**, *460*, 876.

[187] A. S. Keys, S. C. Glotzer, *Phys. Rev. Lett.* **2007**, *99*, 235503.

[188] D. V. Talapin, E. V. Shevchenko, M. I. Bodnarchuk, X. Ye, J. Chen, C. B. Murray, *Nature* **2009**, *461*, 964.

[189] A. Haji-Akbari, M. Engel, A. S. Keys, X. Y. Zheng, R. G. Petschek, P. Palffy-Muhoray, S. C. Glotzer, *Nature* **2009**, *462*, 773.

[190] T. Chen, Z. Zhang, S. C. Glotzer, *Proc. Natl. Acad. Sci. USA* **2007**, *104*, 717; T. Chen, Z. Zhang, S. C. Glotzer, *Langmuir* **2007**, *23*, 6598.

[191] E. Jankowski, S. C. Glotzer, *J. Chem. Phys.* **2009**, *131*, 104104.

[192] A. Troisi, V. Wong, M. A. Ratner, *Proc. Natl. Acad. Sci. USA* **2005**, *102*, 255.

[193] M. Born, E. Wolf, *Principles of Optics: Electromagnetic Theory of Propagation, Interference and Diffraction of Light*, 7th ed., Cambridge University Press, New York, **2001**; W. L. Vos, R. Sprik, A. van Blaaderen, A. Imhof, A. Lagendijk, G. H. Wegdam, *Phys. Rev. B* **1996**, *53*, 16231.

[194] J. Ballato, A. James, *J. Am. Ceram. Soc.* **1999**, *82*, 2273; J. Li, W. Huang, Z. Wang, Y. Han, *Colloids Surf. A* **2007**, *293*, 130.

[195] K. Yoshino, Y. Shimoda, Y. Kawagishi, K. Nakayama, M. Ozaki, *Appl. Phys. Lett.* **1999**, *75*, 932; Y. Shimoda, M. Ozaki, K. Yoshino, *Appl. Phys. Lett.* **2001**, *79*, 3627.

[196] Z.-Z. Gu, T. Iyoda, A. Fujishima, O. Sato, *Adv. Mater.* **2001**, *13*, 1295.

[197] J. Zhou, C. Q. Sun, K. Pita, Y. L. Lam, Y. Zhou, S. L. Ng, C. H. Kam, L. T. Li, Z. L. Gui, *Appl. Phys. Lett.* **2001**, *78*, 661.

[198] Y. Lu, Y. Yin, B. T. Mayers, Y. Xia, *Nano Lett.* **2002**, *2*, 183; J. Ge, Y. Hu, Y. Yin, *Angew. Chem.* **2007**, *119*, 7572; *Angew. Chem. Int. Ed.* **2007**, *46*, 7428; J. Ge, Y. Yin, *Adv. Mater.* **2008**, *20*, 3485; J. Ge, L. He, J. Goebl, Y. Yin, *J. Am. Chem. Soc.* **2009**, *131*, 3484; J. Ge, H. Lee, L. He, J. Kim, Z. Lu, H. Kim, J. Goebl, S. Kwon, Y. Yin, *J. Am. Chem. Soc.* **2009**, *131*, 15687.

[199] J. Ge, J. Goebl, L. He, Z. Lu, Y. Yin, *Adv. Mater.* **2009**, *21*, 4259.

[200] J. M. Weissman, H. B. Sunkara, A. S. Tse, S. A. Asher, *Science* **1996**, *274*, 959; Z. Hu, X. Lu, J. Gao, *Adv. Mater.* **2001**, *13*, 1708;

J. D. Debord, L. A. Lyon, *J. Phys. Chem. B* **2000**, *104*, 6327; M. Kumoda, M. Watanabe, Y. Takeoka, *Langmuir* **2006**, *22*, 4403.

[201] K. Lee, S. A. Asher, *J. Am. Chem. Soc.* **2000**, *122*, 9534; M. M. W. Muscatello, S. A. Asher, *Adv. Funct. Mater.* **2008**, *18*, 1186.

[202] J. H. Holtz, S. A. Asher, *Nature* **1997**, *389*, 829; H. Saito, Y. Takeoka, M. Watanabe, *Chem. Commun.* **2003**, 2126.

[203] Y. Takeoka, M. Watanabe, *Langmuir* **2003**, *19*, 9554.

[204] S. A. Asher, V. L. Alexeev, A. V. Goponenko, A. C. Sharma, I. K. Lednev, C. S. Wilcox, D. N. Finegold, *J. Am. Chem. Soc.* **2003**, *125*, 3322; A. C. Sharma, T. Jana, R. Kesavamoorthy, L. Shi, M. A. Virji, D. N. Finegold, S. A. Asher, *J. Am. Chem. Soc.* **2004**, *126*, 2971.

[205] Y. Iwayama, J. Yamanaka, Y. Takiguchi, M. Takasaka, K. Ito, T. Shinohara, T. Sawada, M. Yonese, *Langmuir* **2003**, *19*, 977; J. Xia, Y. Ying, S. H. Foulger, *Adv. Mater.* **2005**, *17*, 2463.

[206] P. Jiang, J. Smith, D W, J. M. Ballato, S. H. Foulger, *Adv. Mater.* **2005**, *17*, 179.

[207] A. C. Arsenault, D. P. Puzzo, I. Manners, G. A. Ozin, *Nat. Photonics* **2007**, *1*, 468; D. P. Puzzo, A. C. Arsenault, I. Manners, G. A. Ozin, *Angew. Chem.* **2009**, *121*, 961; *Angew. Chem. Int. Ed.* **2009**, *48*, 943; A. C. Arsenault, H. Miguez, I. Manners, G. A. Ozin, U.S. patent 7364673, **2008**.

[208] S. H. Foulger, P. Jiang, A. Lattam, D. W. Smith, Jr., J. Ballato, D. E. Dausch, S. Grego, B. R. Stoner, *Adv. Mater.* **2003**, *15*, 685; K. Sumioka, H. Kayashima, T. Tsutsui, *Adv. Mater.* **2002**, *14*, 1284.

[209] A. C. Arsenault, T. J. Clark, G. von Freymann, L. Cademartiri, R. Sapienza, J. Bertolotti, E. Vekris, S. Wong, V. Kitaev, I. Manners, R. Z. Wang, S. John, D. Wiersma, G. A. Ozin, *Nat. Mater.* **2006**, *5*, 179.

[210] H. Fudouzi, Y. Xia, *Langmuir* **2003**, *19*, 9653; H. Fudouzi, T. Sawada, *Langmuir* **2006**, *22*, 1365.

[211] H. Kim, J. Ge, J. Kim, S. E. Choi, H. Lee, H. Lee, W. Park, Y. Yin, S. Kwon, *Nat. Photonics* **2009**, *3*, 534.

[212] O. L. J. Pursiainen, J. J. Baumberg, K. Ryan, J. Bauer, H. Winkler, B. Viel, T. Ruhl, *Appl. Phys. Lett.* **2005**, *87*, 101902; B. Viel, T. Ruhl, G. P. Hellmann, *Chem. Mater.* **2007**, *19*, 5673.

[213] O. L. J. Pursiainen, J. J. Baumberg, H. Winkler, B. Viel, P. Spahn, T. Ruhl, *Opt. Express* **2007**, *15*, 9553.

[214] T. Nisisako, T. Torii, T. Takahashi, Y. Yakizawa, *Adv. Mater.* **2006**, *18*, 1152.

[215] N. Engheta, *Science* **2007**, *317*, 1698.

[216] S. E. Bowles, W. Wu, T. Kowalewski, M. C. Schalnat, R. J. Davis, J. E. Pemberton, I. Shim, B. D. Korth, J. Pyun, *J. Am. Chem. Soc.* **2007**, *129*, 8694.

[217] A. Stein, F. Li, N. R. Denny, *Chem. Mater.* **2008**, *20*, 649.

[218] J. H. Song, I. Kretzschmar, *ACS Appl. Mater. Interfaces* **2009**, *1*, 1747.

[219] J. Y. Cheng, C. A. Ross, H. I. Smith, E. L. Thomas, *Adv. Mater.* **2006**, *18*, 2505.